

**IN THE NAME OF ALLAH,  
THE MOST GRACIOUS,  
THE MOST MERCIFUL**



Kingdom of Saudi Arabia  
Ministry of Education  
Majmaah University



# MJHS

## Majmaah Journal of Health Sciences

A Refereed Academic Journal Published Biannually by the  
Publishing and Translation Center at Majmaah Universtiy

---

**Vol. 4 No. (2) November 2016 - Safar 1438H ISSN: 1658 - 645X**

---



**Publishing & Translation Center - MU**

## About the Journal

# Majmaah Journal of Health Sciences

---

### **Vision**

The Majmaah Journal of Health Sciences shall be an international peer reviewed journal, which intends to serve researchers through prompt publication of significant advances, and to provide a forum for the reporting and discussion of news and issues concerning health sciences.

### **Mission**

To lead the debate on health and to engage, inform, and stimulate the academicians, researchers, and other health professionals in ways that will improve outcomes for patients.

### **Objectives**

To promote research & evidence based practice in health sciences, so that a firm scientific knowledge base is developed, from which more effective practice may be evolved.

To ensure that the results of the research are rapidly disseminated to the practicing clinicians and educators, in a fashion that conveys their significance for knowledge, culture and daily life.

---

### **Correspondence and Subscription**

**Majmaah University, Post Box 66, AlMajmaah 11952, KSA**

**(email: [mjhs@mu.edu.sa](mailto:mjhs@mu.edu.sa) website: [mjhs.mu.edu.sa](http://mjhs.mu.edu.sa))**

---

### **© Copyrights 2016 (1438 H) Majmaah University**

All rights reserved. No part of this Journal may be reproduced in any form or any electronic or mechanical means including photocopying or recording or uploading to any retrieval system without prior written permission from the Editor-in-Chief.

**All ideas herein this Journal are of authors and do not necessarily express about the Journal view**

# **Majmaah Journal of Health Sciences**

## **Editorial Board**

### **Editor-in-Chief**

**Prof. Mohammed H.S. Al-Turaiki**  
**Professor of Biomedical Engineering & Rehabilitation**  
**College of Applied Medical Sciences**  
**Majmaah University**

### **Members**

**Dr. Nagi Ibrahim Ali Ibrahim**  
**Associate Professor of Nuclear Medicine**  
**College of Applied Medical Sciences**  
**Majmaah University**

**Dr. Khalid Tohami**  
**Assistant Professor of Community Medicine**  
**College of Medicine**  
**Majmaah University**

**Prof. S.Karthiga Kannan**  
**Professor of Oral Medicine & Radiology**  
**College of Dentistry, Al Zulfi**  
**Majmaah University**

**Prof. Santharaj Balakrishnan**  
**Professor of Medical Physics**  
**College of Applied Medical Sciences**  
**Majmaah University**

**Dr. Elsadig Yousif Mohamed Albadawi**  
**Associate Professor of Community Medicine**  
**College of Medicine**  
**Majmaah University**



## Editorial

From the Editor's Desk...

Salaam Alaikum,

It's a pleasure to address you all through this issue of MJHS, I am very happy to pen few words for this issue. It is rightly said by Benjamin Franklin as "either write something worth reading or do something worth writing". There are different rules for reading, for thinking and for talking. Writing blends all three of them.

At the outset let me thank the Rector, **Dr. Khalid bin Saad Al Meqrin** and the Vice Rector for Graduate Studies and Scientific Research **Prof. Dr. Mohammad Bin Abdullah Al-Shaaya'a** for entrusting me with this responsibility of developing and bringing out the prestigious journal of our university, which I hope is fulfilled with all the coordinated efforts from the editorial team. I am pleased to receive many scientific articles from authors belonging to various universities inside and outside the kingdom for our journal that is good news from the point of journal's progression in the right direction. Reading and writing are life skills that everyone should have the opportunity to learn and MJHS is one such platform for academicians inside and outside kingdom.

The editorial team strongly believes that this issue of MJHS will be a useful reference study material for undergraduate and postgraduate student community of medicine and health sciences. The clinical research, case series and case reports stimulate the students to pursue research projects. This reminds me the famous quote "One who studies medicine without books sails an uncharted sea, but he who studies medicine without patients does not go to sea at all" – Sir William Osler.

Good news is that our journal is one step away from getting indexed in popular academic search engines like Copernicus. I hope in near future our journal will achieve the landmark of being indexed in Pubmed. I like to extend my whole hearted thanks to the members of the editorial team for their untiring efforts in bringing this issue in proper form and on time. Also like to thank the reviewer's for their time bound completion of task. As the chief of editorial team I thank all the authors for submitting their original work to our journal.

**Editor-in-Chief, MJHS**

**Professor. Dr. Mohammed HS Al-Turaiki**



# Contents

Editorial ..... vii

## ORIGINAL ARTICLES

**Tuberculosis Trend in Majmaah, Saudi Arabia: A 10 Year Retrospective Study  
(2005-2014)**

*Elsadig Y. Mohamed, Gopikrishnan Muraleedharan, Khaled A. Medan, Waqas S. Mahmoud, Sawsan M. Abdalla1, Mohamed A Al Mansour, Talal S. Algahmdi ..... 1*

**Prevalence of Helicobacter pylori and its association with chronic diseases in  
Al-Majmaah population**

*Khalid M Aljarallah ..... 11*

**Comparative study of morphology, elemental constitution and crystal structure  
of two large sialoliths: by way of scanning electron microscope energy  
dispersive x-ray (EDS) and x-ray diffraction (XRD) analysis**

*Bindu Das. R, Deepti Simon, C.R.Sobhana, Akhilesh A.V ..... 20*

**Cystic oral lesions of salivary gland origin in children**

**Case series – An Observational study**

*S.Karthiga Kannan, J. Eugenia Sherubin, M.S. Priya, Mouetaz Kheirallah, Salama M.H ...28*

**Detection of Retinal Blood Vessels by using Gabor filter with Entropic threshold**

*Mohamed. I. Waly, Ahmed El-Hossiny ..... 36*

**Convex Optimization for Energy Efficiency of a Bluetooth Based Wearable  
Continuous Cardiac Monitoring Node**

*Jaspal Singh and Santhanaraj Balakrishnan ..... 56*

## CASE STUDY

**Management of Signet-Ring Cell Carcinoma of the Rectum**

**A Case Study**

*Majed Alamri and Helen Cecily ..... 64*

# Contents

<b>Proposal Application Requirement and Application .....</b>	<b>83</b>
<b>Conferences 2017 .....</b>	<b>84</b>

ORIGINAL ARTICLE

## Tuberculosis Trend in Majmaah, Saudi Arabia: A 10 Year Retrospective Study (2005-2014)

Elsadig Y. Mohamed<sup>1</sup>, Gopikrishnan Muraleedharan<sup>2</sup>, Khaled A. Medan<sup>3</sup>, Waqas S. Mahmoud<sup>4</sup>, Sawsan M. Abdalla<sup>1</sup>, Mohamed A Al Mansour<sup>5</sup>, Ahmed Khalid Al-Salbud, Abdulkreem Al-Naseer<sup>6</sup>

1 Associate Professor of Community Medicine, College of Medicine, Majmaah University, Saudi Arabia

2 Lecturer in Medical informatics, College of Medicine, Majmaah University

3 Assistant professor of Community Medicine, College of Medicine, Majmaah University, Saudi Arabia

4 Lecturer, Biostatistics, Department of Public Health & Community Medicine, College of Medicine, Majmaah University, Saudi Arabia

5 Assistant professor of Family Medicine, College of Medicine, Majmaah University, Saudi Arabia

6 Student, College of Medicine, Majmaah University

Correspondence: Elsadig Yousif Mohamed: College of Medicine, Majmaah University, Saudi Arabia.

Email: ey.mohamed@mu.edu.sa - elsadigoo@gmail.com. Tel. 00966 530748432,

Fax. +966164042318, P.O.Box 66

Received on: 9th October, 2016; Accepted on: 1st November, 2016

### Abstract

**Objectives:** The objective of the current study was to determine the epidemiology and characteristics of tuberculosis in Majmaah, Saudi Arabia during 2005-2014.

**Patients and methods:** Retrospective observational descriptive study of data obtained from the Tuberculosis Information System. All medical records of tuberculosis patients registered during the study period were reviewed after obtaining the ethical approval. The data were collected by a check list and analyzed by SPSS.

**Results:** Total TB reported incidence decreased from 8:100,000 to 6:100,000 populations between 2005 and 2014. The reported incidence of the disease was higher (32.8%) among the age group (25 and 34) years. The female gender was mostly affected (52.8%) compared to males. Extra pulmonary and new TB cases were (67.2%) and (98.5%) respectively. Twenty two patients (32.8%) were tested for HIV/AIDS and all of them were negative. Regarding treatment outcome, ten patients (14.9%) cured, 34 (50.7%) completed treatment, 15 (22.4%)

### الملخص

**الأهداف:** تمثلت أهداف الدراسة في تحديد وبائية وخصائص مرض الدرن بالجمعة- المملكة العربية السعودية في الفترة من ٢٠٠٥ وحتى ٢٠١٤.

**منهجية الدراسة:** هذه دراسة وصفية استرجاعية للدرن بمنطقة المجمعة من واقع السجلات الخاصة بنظم معلومات الدرن. تمت دراسة السجلات الطبية لمرضى الدرن المسجلين خلال فترة الدراسة وهي عشر سنوات بعد الحصول على الموافقة الأخلاقية. تم جمع البيانات عن طريق قائمة المراجعة كما تم التحليل بواسطة برنامج الحزمة الاحصائية للعلوم الاجتماعية.

**النتائج:** انخفض معدل حدوث حالات الدرن بالمجمعة من ٨:١٠٠٠٠٠ إلى ٦:١٠٠٠٠٠ من السكان بين عامي ٢٠٠٥-٢٠١٤. أوضحت الدراسة أن معدل حدوث الحالات أعلى (٣٢,٨٪) في الفئة العمرية (٢٥-٣٤) سنة مقارنة ببقية الفئات العمرية كما أن الإناث هم الأكثر إصابة بالمرض (٥٢,٨٪) مقارنة بالذكور. يمثل الدرن خارج الرئة والاصابات الحديثة (٧٦,٢٪) و (٩٨,٥٪) على التوالي. تم التحليل لعدد ٢٢ (٣٢,٨٪) من المرضى للكشف عن مرض الأيدز حيث أثبت التحليل أن جميعهم خاليين من

transferred and 4 (6%) defaulted; the death ratio was 6%.

**Conclusion:** Tuberculosis reported incidence declined in Majmaah, Saudi Arabia during 2005 and 2014; however the disease reported incidence increased among the expatriates compared to Saudi population. During the study period, tuberculosis was more common among females, younger age groups, illiterates and married population.

**Key words:** Tuberculosis trends; incidence; retrospective study

المرض. بالنسبة للعلاج وجدت الدراسة أن (٩, ١٤) % شفوا تماماً (٧, ٥٠) % أكملوا العلاج و (٤, ٢٢) % تم تحويلهم بينما (٦) % تخلفوا ولم يكملوا العلاج. معدل الوفاة بالنسبة للدرن بالمجمعة هو ٦ %.

الخلاصة: انخفض معد لحداث حالات الدرن بالمجمعة- بالمملكة العربية السعودية خلال ٢٠٠٥-٢٠١٤ الا أن هنالك زيادة ملحوظة في معدل الاصابة بالمرض وسط الأجانب مقارنة بالسعوديين. خلال سنوات الدراسة كانت الاصابة بالدرن أعلى بين الاناث والسكان الأقل عمرا وغير المتعلمين بالإضافة الى المتزوجين مقارنة بنظرائهم.

## Introduction

Tuberculosis (TB) is an infectious disease caused by the bacillus *Mycobacterium tuberculosis*. The disease typically affects the lungs (pulmonary TB) but can affect other parts of the body as well (extra pulmonary TB) <sup>1</sup>. Despite the availability of highly effective treatment of the disease for decades, TB remains a major global health problem. Globally, there were an estimated 9.0 million incident cases and 1.5 million deaths due to tuberculosis in 2013<sup>2</sup>, most of the cases were in the South-Eastern Asia, African and Western Pacific regions (35%, 30% and 20%) respectively<sup>3,4</sup>. Tuberculosis is highly prevalent in the Eastern Mediterranean Region; the prevalence rate is estimated at 18:100 000 population 2012<sup>5</sup>.

In Saudi Arabia, tuberculosis remains a public health threat despite improved living standards and public awareness, availability of free anti tuberculosis medications, and implementation of BCG vaccination at birth<sup>6</sup>. In 2007, the World Health Organization estimated the incidence of TB in the Kingdom as

46:100,000 population/year; the incidence of smear positive TB as 21:100 000 populations/year and the prevalence of all forms of TB as 65:100,000 population/year <sup>7</sup>.

During 1991-2010 there were a total of 64,345 reported TB cases in Saudi Arabia, non-Saudis had 2-3 times higher incidence than the expatriates. The disease trend was rising over the first 10 years of the study period then it started to fall slightly. The incidence increased with age, but only people older than 45 years showed a declining trend. Regional variations were observed; Makkah and Jazan regions had the highest incidence rates while rising trend was observed in Makkah and the central regions <sup>8</sup>.

The kingdom is facing increased trends in resistance to pulmonary tuberculosis treatment <sup>9</sup>, a retrospective study was conducted which included patients with culture proven diagnosis of tuberculosis seen at King Khalid National Guard Hospital, Jeddah showed treatment failure rate as 30.6%. Noncompliance and drug resistance

were considered the main two factors which were significantly associated with treatment failures<sup>10</sup>.

In 1992, the Ministry of Health established a National Tuberculosis Control Committee to implement a control program throughout the Kingdom, and in 1999 the MOH implemented the Direct Observed Treatment Short course (DOTS) strategy recommended by the WHO. This strategy was adopted in the kingdom in 1998, and an expansion phase was established to include all the provinces in the year 2000<sup>11</sup>.

In Saudi Arabia there are several institutions providing healthcare for patients with tuberculosis: the National Guard, Military, Security Forces and Ministry of Health hospitals. Patients attending the private sector suspected of having TB are referred to government hospitals<sup>12</sup>.

Saudi Arabia underwent a vast economic expansion which led to improving social and health services. This was associated with an influx of up to six million expatriates; most of them were from high burden TB countries such as India, Pakistan, Bangladesh, Indonesia and Yemen. The kingdom is facing increased trends in resistance to pulmonary tuberculosis treatment since most of the expatriates and pilgrims coming from countries with high prevalence of multi and extensive drug resistance tuberculosis (MDR-TB and XDR-TB)<sup>13,14</sup>.

The objectives of the current study were to determine the trends of tuberculosis reported incidence rate in Majmaah, Saudi

Arabia during 2005-2014; to determine the relation between tuberculosis trends and the patients' social factors and to specify treatment outcome for tuberculosis patients during the study period.

## Patients and methods

Study design:

A descriptive retrospective study to determine the reported incidence trends of tuberculosis in Majmaah, Saudi Arabia in the period 1 January 2005 to 31 December 2014. Study population and setting:

Majmaah is located in Riyadh region, 180 Km from the capital city of Saudi Arabia. All TB suspects from the area are referred to the department of pulmonary diseases in King Khaled hospital, Majmaah. All medical records of tuberculosis patients registered from 2005 to 2014 in the hospital were reviewed and included in this study. The data were verified from the records of King Saud Chest Hospital in Riyadh where all the data of TB patients from Majmaah were kept.

Data collection and analysis:

The data were collected by a pre-tested check list contained social factors (patient's age, gender, nationality and residence). It also included TB classification, type of treatment and treatment outcome. Tuberculosis treatment was assessed according to WHO guidelines. The data collectors were trained to improve the quality of data collection. The data was edited, cleaned, summarized using a master sheet and double entered into the software. The SPSS for Windows

software, version 20 (SPSS, Chicago, Illinois, USA) was employed to analyze the data. Descriptive statistics was used (frequency and standard deviation). Comparisons between groups were made using the chi-squared test. P value < 0.05 was considered significant and all tests were 2-sided. The ethical approval was obtained from the ethical committee of the Basic Health Research Center, Majmaah University. The data was kept confidential and was utilized only for the purpose of this study.

## Results

There were a total of 67 TB cases reported to King Khaled Hospital, Majmaah during

2005-2014. Of these, 10 (14.9%) were from the age group 0-14 years. The age groups (15-24), (25-34), (35-44) and more than 44 years constituted 16.4%, 32.8%, 13.5% and 22.4% respectively. Most of the cases (89.6%) were illiterate; the others (10.4%) had a general education. Most of the TB cases (56.7%) were from urban areas and more than half (50.8%) were married. Most of the TB patients were Saudi 36 (53.7%); the non-Saudi were 31 (46.3%).

Table (2) shows the characteristics of tuberculosis in Majmaah. Most of TB cases 45 (67.2%) were extra pulmonary. Pulmonary tuberculosis cases were 22 (32.8%). Almost all patients 66 (98.5%) were new cases;

**Table (1). Social characteristics of the TB patients n=67**

Social characteristics	No.	Percent
<b>Age/ years:</b>		
0 -14	10	14.9
15- 24	11	16.4
25-34	22	32.8
35-44	9	13.5
More than 45	10	22.4
<b>Gender:</b>		
Male	32	47.8
Female	35	52.2
<b>Education:</b>		
Illiterate	60	89.6
General	7	10.4
<b>Residence:</b>		
Urban	38	56.7
Rural	29	43.3
<b>Marital status:</b>		
Single	25	37.3
Married	34	50.8
Divorced/ Widowed	8	11.9
<b>Nationality:</b>		
Saudi	36	53.7
Non-Saudi	31	46.3

- Mean age in the first five years= 33.7 years
- Mean age in the second five years= 31.1 years
- Total Mean age= 32 years

only one case was a relapse (1.5%). Most TB diagnosis was based on ICT (50.7%), culture (23.9%), sputum (22.4%) and XR (3.0%). Twenty two patients (32.8%) were tested for HIV/AIDS and all of them were negative. Regarding treatment outcome, ten patients (14.9%) cured, 34 (50.7%) completed treatment, 15 (22.4%) transferred and 4 (6%) defaulted. The death ratio was 6%.

Fig (1) Shows tuberculosis trends in Majmaah during 2005 and 2014. In all, total TB reported incidence decreased from 8:100,000 to 6:100,000 populations. Smear positive TB in 2005 was 2:100,000; no smear positive TB case was reported in 2014.

Table (3) shows TB Trends according to social characteristics between the first and the second five year terms (2005-2009 and 2010-2014). Overall, only one case dropped in total between the first and the second terms. The number of tuberculosis patients in the age group 0-34 years increased from 21 to 22 cases while reduces from 13 to 11 cases in the age group 35 years and more. Regarding gender, the number of males remained the same as 16 cases between the years 2005-2009 and 2010-2014. For the females, the number of cases reduced by one case from 18 to 17 cases between the two terms. The number of Saudi TB cases reduced by 50% between the

**Table (2). Characteristics of Tuberculosis**

Characteristics	No.	Percent
<b>Type of TB:</b>		
Pulmonary	22	32.8
Extra pulmonary	45	67.2
Total	67	100.0
<b>Patient type:</b>		
New	66	98.5
Relapse	1	1.5
Total	67	100
<b>Means of diagnosis:</b>		
ICT	34	
Sputum	16	50.7
Culture	15	23.9
XR	2	22.4
Total	67	3.0
		100.0
<b>HIV status:</b>		
Negative	22	32.8
Not tested	45	67.2
Total	67	100
<b>Treatment outcome:</b>		
Cured	10	14.9
Completed	34	50.7
Transferred out	15	22.4
Defaulted(Loss to follow up)	4	6.0
Died	4	6.0
Total	67	100

### CASES/100 000 POPULATIONS 2005 - 2014

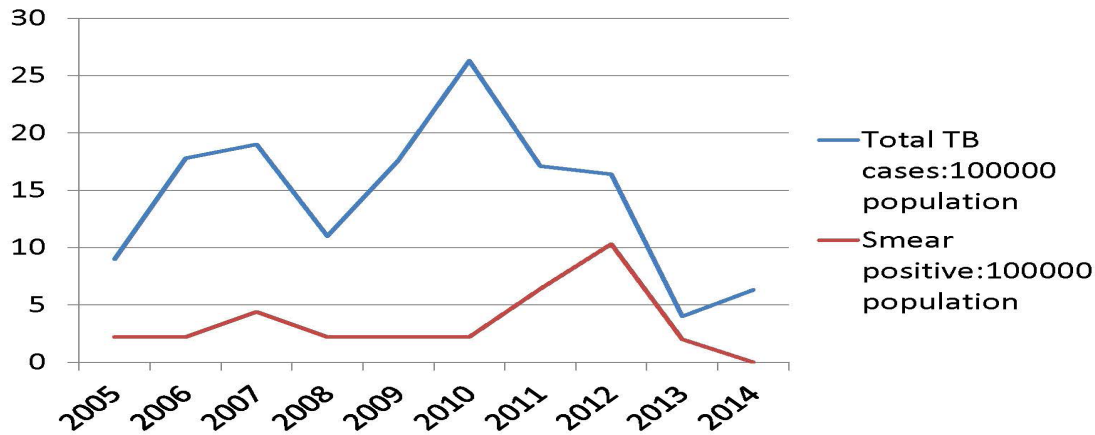


Fig (1) Tuberculosis reported incidence in Majmaah 2005-2014

Table (3). TB Trends according to social characteristics

Social characteristic	Cases/years		Total	p
	(2005-2009)	(2010-2014)		
<b>*Age/ years:</b>				
Less than 35	21(48.8%)	22(51.2%)	43 (64.2%)	0.4
35 and more	13(54.2%)	11(45.8%)	24(35.8%)	
Total	34 (50.7%)	33(49.3%)	67(100.0%)	
<b>Gender:</b>				
Male	16 (50.0%)	16(50.0%)	32 (47.8%)	0.84
Female	18(51.4%)	17(48.6%)	35(52.2%)	
Total	34(50.7%)	33(49.3%)	67(100.0%)	
<b>Nationality:</b>				
Saudi	24(66.7%)	12(33.3%)	36(53.8%)	<0.001
Non-Saudi	10(32.3%)	21(67.7%)	31(46.2%)	
Total	34(50.7%)	33(49.3%)	67(100.0%)	

first and second five years of the study. On the other hand the expatriates TB cases were doubled during the two terms.

#### Discussion:

Sixty seven cases were diagnosed as tuberculosis by passive case finding in Majmaah area during 2005-2014. The most age group who had the higher reported

incidence was between 25 and 34 years while the mean age was 32 years. The mean age of tuberculosis according to this study was less for the second term compared to the first term; this indicates that the disease is moving towards the young generations. This finding is in line with the global trend of the disease<sup>15</sup>. The males were more affected by the disease compared to females (52.2% Vs 47.8%). This

finding supports studies conducted in Spain, India and Saudi Arabia<sup>16,17, 18, 20</sup>.

Most TB cases reported during the study period were extra-pulmonary. This finding is in line with Alrajhi et al who conducted a study in King Faisal Specialist hospital and Research Centre and reported higher prevalence of extra-pulmonary tuberculosis of 58% compared to pulmonary tuberculosis<sup>21</sup>. It also agrees with W.H.O. that the western part of the gulf region, which includes Saudi Arabia, has a high prevalence of extra-pulmonary tuberculosis<sup>22</sup>. However; it contradicts TB trends in Iran and Qatar<sup>23,24</sup>. This finding also contradicts Al-Orainey I et al who found that most cases of TB (73%) in Saudi Arabia were pulmonary tuberculosis<sup>25</sup>. Presence of extra pulmonary TB is of lower epidemiological importance since the infection is confined to the patient and can't be transmitted to others. Almost all TB patients according to this study were new cases. This finding is in agreement with studies elsewhere<sup>26, 20</sup>. According to this study, treatment success rate was low (65.6%). Sammana Y et al and Al-Hajoj S. et al reported higher success rate as 81% and 69.4% in Saudi Arabia respectively<sup>27, 12</sup>. Fifteen patients (22.4%) were transferred out. This high rate of transfer may be due to the fact that patients who were diagnosed as tuberculosis were transferred out of the country after initiating treatment. In this analysis no patient was recorded as treatment failure. All TB patients who were tested for HIV were negative 22 (32.8%): However 45 (67.2%) patients were not tested. In Saudi Arabia the prevalence of

HIV among TB patients was 3.3%. Screening for HIV in tuberculosis patients remains underutilized despite the increase of HIV/AIDS among Saudi nationals<sup>21, 28</sup>. The death ratio from all forms of TB in this study was 6% which was the same as reported by others<sup>29, 20</sup>.

The prevalence of TB during the study period did not exceed in any year the national prevalence of the disease which is around 18:100,000 populations that classify the kingdom as an average TB burden country<sup>8,30</sup>. This trend is in line with a decrease incidence in Riyadh region of Saudi Arabia between 2000-2009<sup>18</sup>. This decline is also in line with the global trend of tuberculosis since the year 2000<sup>19</sup>. Contrary to our findings, Gleason JA reported an increase incidence of the disease all over the kingdom including the central region which showed a significant rise from 6.4 to 14.2/100,000 over 1991 and 2010<sup>31</sup>. It also contradicts Al Hajooj S et al who found that the disease showed an upward trend among both Saudi and non-Saudi population<sup>20, 12</sup>.

In general the decline trend of the disease among Saudi and increase trend among non-Saudi ( $\pi < .001$ ) is consistent with TB trends in Saudi Arabia shown by Al-Orainey et al<sup>25</sup> and Abouzeid MS et al<sup>18</sup>. This may be explained by the fact that most of the non-Saudi working force is coming from high TB burden countries<sup>18</sup>.

Conclusion:

Tuberculosis reported incidence was declining in Majmaah, Saudi Arabia during 2005 and

2014: however the disease is increasing among the expatriates. The disease was more common among the females, the younger age groups, the illiterates and the married population. Most of TB cases were extra-pulmonary and almost all were new. The treatment success rate was low. All TB patients presented to the health services and tested for HIV were negative: However most of the cases were not tested for HIV.

#### **Acknowledgement:**

The authors would like to acknowledge the Deanship of Scientific Research as well as the Basic and Health Research Center, Majmaah University for supporting this work. We would like to acknowledge King Khaled hospital in Majmaah for their support.

Financial support and sponsorship:

This work was supported by the Deanship of Scientific Research, Majmaah University, Saudi Arabia.

#### **Conflicts of interest:**

There are no conflicts of interest regarding this research

#### **References:**

1. K. Park. Park's textbook of preventive and social medicine. 20<sup>th</sup> edition. India: M/s Banarsidas Bhanot publishers. 2009:159
2. World Health Organization (WHO) 2014. Global tuberculosis report 2014. WHO/HTM/ TB/ 2014.8, Geneva, Switzerland: WHO, 2014
3. WHO 2009. 13<sup>th</sup> annual report on global control of tuberculosis. Global tuberculosis control epidemiology, strategy and financing. WHO/HTM/TB/2013.411. Geneva: WHO, 2009
4. Dye C, Maher D, Weil D, Espinal M, Raviglione M. Targets for global tuberculosis control. *Int J Tuberc Lung Dis.* 2006; 10:460-2
5. World Health Organization (WHO) 2013. Global tuberculosis report, 2013. WHO/HTM/TB/2013.11, Geneva, York, Paris: WHO, 2013
6. Al-Hajaj MS, Pandya L, Mari AA, Madani A, Al-Sharif N, Almajed S. Pulmonary tuberculosis in Saudi Arabia: a retrospective study of 1566 patients. *Ann Saudi Med.* 1991
7. World Health Organization (WHO) 2007. Global tuberculosis control report 2007. WHO/HTM/TB/2007.11. Geneva, New York and Paris: WHO, 2013
8. Al-Orainey I, Alhedaithy MA, Alanazi AR, Barry MA, Almajid FM. Tuberculosis incidence trends in Saudi Arabia over 20 years: 1991-2010. *Annals of Thoracic Medicine* 2013; 8 (3): 148-152
9. Khan MY, Kinsara AJ, Osoba AO, Wali S, Samman Y, Memish Z. Increasing resistance of M. tuberculosis to anti-TB drugs in Saudi Arabia. *Int J Antimicrob Agents.* 2001; 17(5):415-8.
10. Al-Hajoj S1, Varghese B, Shoukri MM, Al-Omari R, Al-Herbwai M, Alrabiah F, et al. Epidemiology of anti-tuberculosis drug resistance in Saudi Arabia: findings of the first national survey. *Antimicrob Agents*

- Chemother. 2013 May; 57(5):2161-6.  
doi: 10.1128/AAC.02403-12. Epub 2013 Mar 4
11. Haldal E, Kuyvenhoven JV, Wares F, Migliori GB, Ditiu L, Fernandez de la Hoz K, et al. Diagnosis and treatment of tuberculosis in undocumented migrants in low- or intermediate-incidence countries. *Int J Tuberc Lung Dis.* 2008; 12:878–888
  12. Al-Hajoj SA. Tuberculosis in Saudi Arabia: Can we change the way we deal with the disease? *Journal of Infection and Public Health* 2010; 1-8doi: 10/1016/j.jiph.2009.12.001  
From: <http://www.researchgate.net/publication/45628794>
  13. Wilder-Smith A, Foo W, Earnest A, Paton NI. High risk of Mycobacterium tuberculosis infection during the Hajj pilgrimage. *Trop Med Int Health* 2005; 10:336-339
  14. Al-Orainey IO. Tuberculosis infection during Hajj pilgrimage: The risk to pilgrims and their communities. *Saudi Med J* 2013; 34: 676-80
  15. World Health Organization (WHO) 2006. Tuberculosis fact sheet number 104 (updated October 2015).  
From: <http://www.who.int/mediacentre/factsheets/fs104/en> (Accessed on 10.11.2015)
  16. Cruz-Ferro E, Ursúa-Díaz MI, Taboada-Rodríguez JA, Hervada-Vidal AX, Anibarro L, Túnuez V. Epidemiology of tuberculosis in Galicia, Spain, 16 years after the launch of the Galician tuberculosis program. *Int J Tuberc Lung Dis* 2014; 18(2):134–140
  17. Sharma SK, Goel A, Gupta SK, Mohan K, Sreenivas V, Rai SK, et al. Prevalence of tuberculosis in Faridabad district, Haryana State, India. *Indian J Med Res.* 2015; 141(2):228-35.
  18. Abouzeid MS, Zumla AI, Felemban Sh, Alotaibi B, Grady JO and Memish ZA. Tuberculosis Trends in Saudis and Non-Saudis in the Kingdom of Saudi Arabia – A 10 Year Retrospective Study (2000–2009). *PLoS One.* 2012; 7(6): e39478. doi: 10.1371/journal.pone.0039478
  19. World Health Organization (WHO) 2015. Health in 2015: from MDGs, Millennium Development Goals to SDGs, Sustainable Development Goals. WHO/HTM/TB/2015.114, Switzerland and France: WHO, 2015  
From: [www.who.int/about/licensing/copyright\\_form/en/index.html](http://www.who.int/about/licensing/copyright_form/en/index.html)
  20. Al-Hajoj S, Varghese B. Tuberculosis in Saudi Arabia: the journey across time. *J Infect Dev Ctries* 2015; 9(3):222-231.
  21. Alrajhi AA, Nematallah A, Abdulwahab S, Bukhary Z. Human immunodeficiency virus and tuberculosis co-infection in Saudi Arabia. *East Mediterr Health J.* 2002; 8(6):749-53.
  22. World health organization (2013) Global tuberculosis Report 2013. Geneva: WHO. WHO/HTMTB/2013.11 From: <http://apps.who.int/iris>
  23. Abu Khattab M, Khan FY, Al Maslamani M, Al-Khal AL, El Gendy A, Al

- Soub H, et al. Pulmonary and Extra Pulmonary Tuberculosis in Qatar: A First Retrospective Population-Based Study. *Advances in Infectious Diseases* 2015; 5:148-153 <http://dx.doi.org/10.4236/aid.2015.54018>
24. Babamahmoodi F, Alikhani A, Charati JY, Ghovvati A, Ahangarkani F, Delavarian L, et al. Clinical Epidemiology and Paraclinical Findings in Tuberculosis Patients in North of Iran. *BioMed Research International* 2015; Volume 2015: 1-5 <http://dx.doi.org/10.1155/2015/381572>
25. Al-Orainey I, Alhedaihy MA, Alanazi AR, Barry MA, and Almajid FM. Tuberculosis incidence trends in Saudi Arabia over 20 years: 1991-2010. *Ann Thorac Med*. 2013 Jul-Sep; 8(3): 148–152. doi: 10.4103/1817-1737.114303
26. Liew SM, Khoo EM, Ho B K, Lee YK, Mimi O, Fazlina MY, et al. Tuberculosis in Malaysia: predictors of treatment outcomes in a national registry *The International Journal of Tuberculosis and Lung Disease* 2015; 19 (7): 764-771
27. Sammana Y, Krayema A, Haidara M, Mimesha S, Osobab A, Al-Mowaalladb A, et al. Treatment outcome of tuberculosis among Saudi nationals: role of drug resistance and compliance. *Clinical Microbiology and Infection* 2003; 9 (4): 289–294
28. Mazroa MA, Kabbash IA, Felemban SM, Stephens GM, Al-Hakeem RF, Zumla AI, et al. HIV case notification rates in the Kingdom of Saudi Arabia over the past decade (2000-2009). *PloS one* 7: e45919.
29. Abouzeid MS, Al Hakeem RF, Memish ZA. Mortality among tuberculosis patients in Saudi Arabia (2001-2010). *Ann Saudi Med* 2013; 33(3): 247-252 DOI: 10.5144/0256-4947.2013.247
30. Varghese B, Al-Omari R, Al-Hajoj S. Inconsistencies in drug susceptibility testing of *Mycobacterium tuberculosis*: Current riddles and recommendations. *Int J Mycobacteriol*. 2013; 2: 14-17
31. Gleason JA, McNabb SJ, Abduljadayel N, Abouzeid MS, Memish ZA. Tuberculosis trends in the Kingdom of Saudi Arabia, 2005 to 2009. *Ann Epidemiol*. 2012; 22(4): 264-9. doi: 10.1016/j.annepidem.2012.01.007. Epub 2012 Feb 24.

ORIGINAL ARTICLE

## Prevalence of Helicobacter pylori and its association with chronic diseases in Al-Majmaah population

Khalid M Aljarallah\* (PhD)

(\* ) Medical Laboratories Sciences Dept., College of Applied Medical Sciences, Majmaah University

Received on: 7th October, 2016; Accepted on: 7th November, 2016

### Abstract

Background: A retrospective and descriptive study of confirmed Helicobacter pylori (HP) cases was observed for the prevalence of HP infection in Majmaah area with respect to age and gender of the subjects and seasonal variation. Furthermore, the association of HP with a number of other chronic diseases was also correlated.

Methodology: Data for 276 confirmed HP cases were retrieved from King Khalid Hospital (KKH) in Majmaah City (Riyadh Pegin, KSA) between 2011 and 2015 and analyzed retrospectively with respect to the gender and age of the patients and seasonal variation in HP prevalence in different months of the year was also observed. Association of HP with other chronic diseases like diabetes and hypertension was also investigated. Descriptive and inferential statistics were also calculated for all data.

Results: This retrospective descriptive study revealed that prevalence of HP during five years, there were 276 HP confirmed cases. On an average, most cases were diagnosed during the first five calendar months, starting from January through May. The maximum number of 38 cases of HP infection was observed in May followed by 36 cases in March. On the other hand, the minimum number of cases was

### الملخص

قامت هذه الدراسة برصد حالات الإصابة السابقة بميكروب جرثومة المعدة في منطقة المجمععة ومدى تلازمها مع الفئة العمرية و الجنس اضافة لعلاقة الاصابات باختلاف المواسم . اضافة لذلك تم دراسة تلازم الإصابة بالميكروب مع أمراض مزمنة معينة

طريقة العمل : تم رصد ٢٧٦ حالة مصابة بجرثومة المعدة من خلال سجلات مستشفى الملك خالد بمحافظة المجمععة للفترة الممتدة من عام ٢٠١١ الى عام ٢٠١٥ مع تحليل هذه النتائج وربطها بجنس المصاب وفئته العمرية وموسم حدوث الإصابة خلال أشهر السنة. كما تم استقراء مدى التلازم بين تلك الاصابات ووجود أمراض مزمنة لدى المصابين خاصة مرض السكري وارتفاع ضغط الدم . وتم اجراء التحليل الاحصائي لكافة النتائج.

النتائج : أظهرت نتائج هذه الدراسة الوصفية الاستقرائية لظهور الإصابة بجرثومة المعدة وذلك خلال الفترة الممتدة لخمس سنوات وجود ٢٧٦ حالة إصابة مؤكدة . معظم الحالات تم رصدها خلال الأشهر الخمسة الأولى من يناير وحتى مايو. أعلى متوسط لحالات الإصابة تم رصدها في شهر مايو وبلغت ٣٨ حالة ، تبعها شهر مارس بعدد ٣٦ حالة . ومن جهة أخرى فقد بلغت أدنى حالات الإصابة في شهر يوليو ٦ حالات يليها شهر يونيو بعدد ١٢ حالة .

الخلاصة : من بين مراجعي مستشفى الملك خالد

reported in July with only 6 cases followed by June with 12 cases.

Conclusion: Out of estimated total number of annual visitors (75420) to KKH, 276 symptomatic HP infected patients were confirmed over five years. The number of cases identified was 2, 160, 84, and 30 in the age group 0-14, 15-39, 40-64, and  $\geq 65$  years respectively. Hypertension was found to increase with age, whereas the diabetes was not linear with increasing age.

بالمجمعة والذي يقدر عددهم بخمسة وسبعين ألفاً وأربعمائة وعشرين مريضاً أظهر مئتين وستة وسبعين منهم أعراض الإصابة بجرثومة المعدة خلال مدة الدراسة البالغة خمس سنوات. توزعت حالات الإصابة بعدد بلغ حالتين مئة وستين أربعة وثمانين وثلثين للفئات العمرية ٠-٤، ١٥-٣٩، ٤٠-٦٤ و٦٥ عاماً على التوالي. حالات الإصابة بالميكروب التي تلازمت مع مرض ضغط الدم وجد أنها تزداد بزيادة العمر بينما لم يرصد ذلك في الاصابات المتلازمة مع مرض السكري.

## Introduction

HP is one of the world's most common bacterial infections. It has two to six flagella that give it the mobility to withstand rhythmic gastric muscle contractions and helps it to penetrate the gastric mucosa<sup>(1)</sup>. HP produces urease to create an alkaline environment<sup>(1)</sup>, which enables the organism to survive in the acidic stomach. Colonization usually persists for years or even decades. It is estimated that HP colonizes stomachs of around 50 % of world's population. The world health organization has classified HP as a group 1 carcinogen for gastric adenocarcinoma.<sup>(2)</sup> Although humans are the principal reservoir of this pathogen, closely related similar organisms have also been found in primates.<sup>(1)</sup> Although. The organism is generally acquired during the childhood by the fecal-oral, oral-oral or gastro-oral route<sup>(3)</sup>. Consistent with these transmission routes, these bacteria have been isolated from feces, saliva and dental plaque of some infected people. Transmission occurs mainly within families in developed nations yet can also be acquired from the community in developing countries. HP

may also be transmitted orally by means of fecal matter through the ingestion of waste-tainted water, thus a hygienic environment could help decrease the risk of HP infection.

Antibodies of HP found in human serum are indicators for this infection. Positive HP IgG with high sensitivity and specificity have been reported from various countries for diagnosis of HP infection.<sup>(4)</sup> HP DNA has been detected by polymerase chain reaction in sewage water. It can survive for several days in distilled water; saline and sea water if these are kept cool. However, at room temperature they become non-cultivable after one to three days. It is possible that particulate matter could be providing a more favorable local environment and increases its survival time. Most people (over 80%) infected with HP show no symptoms as these are "silent" and produce no symptoms.

The prevalence of HP infection is not uniform between societies, and it varies both geographically and according to social and ethnic group. This infection around

the world ranges between 20% and 90% in adult populations<sup>(5)</sup> and is more prevalent in developing countries, since it is associated with poverty and social deprivation<sup>(6)</sup>. The prevalence in developing countries ranges between 49.1% and 87% in adults,<sup>(7, 8)</sup> but it is decreasing in some of these countries like South Korea<sup>(13)</sup>, Brazil<sup>(16)</sup> and Japan<sup>(16)</sup>. The main risk factors for HP infection include overcrowded households, poor sanitation and poor water supply.<sup>(6)</sup> However, in developed countries the prevalence ranges from 11% to 32% in adults, and 10% to 16.7% in children<sup>(9, 10)</sup>. During the twentieth century in developed countries, a decrease in prevalence of HP was observed accompanied by a corresponding decrease in the incidence of gastric cancer and peptic ulcer disease.<sup>(11)</sup> Majority of the population of the developing world is infected by HP from an early age. Growing efforts are being placed on developing strategies to reduce the prevalence of the infection in developing countries, because gastric cancer is even more prevalent in these countries.<sup>(12)</sup>

For instance, a recent study in South Korea showed that there had been a significant decrease over the seven-year period from 1998 (66.9%) to 2005 (59.6%).<sup>(13)</sup> The prevalence ranges from 9% to 78.6% among schoolchildren in developing countries,<sup>(14, 15)</sup> and in Brazil it ranges from 2.4% to 66.5%.<sup>(5, 16)</sup> Infection prevalence is higher in socioeconomically deprived communities and lower among individuals of Japanese descent.<sup>(16)</sup>

The prevalence of HP infection in Saudi Arabia has noticeably increased with respect to age. It rose from 32.4% in those aged 5–10 years, more than 66.4% for those aged 20–30 years, and 75% in those over 50 years. On the other hand, reports showed that HP infection prevalence in the country was 68–82.2% in the 1990s.<sup>(17)</sup> With its estimated population in Majmaah city approaching to 133285 (both Saudis and non-Saudis), out of them 77929 are men and 55356 women, Majmaah City can be considered as a representative example of the semi-rural region in Saudi Arabia.

Infection with HP is associated with chronic gastritis and peptic ulceration, and the bacterium is also considered a risk factor for developing gastric adenocarcinoma and mucosa-associated lymphoid tissue (MALT) lymphoma.<sup>(18)</sup> In a study from Saudi Arabia, the well-described association of HP with non-ulcer dyspepsia was confirmed.<sup>(19)</sup>

The relationship between HP infection is often associated with other chronic diseases in humans like diabetes mellitus<sup>(30)</sup>, hypertension<sup>(31)</sup> and obesity<sup>(32)</sup>.

The current study aimed at determining the prevalence of HP in the population of Majmaah city during a period of five years between 2011 and 2015.

## Methodology

This study is a retrospective cross-sectional study, of all proved cases of HP in King Khalid Hospital - Majmaah - Riyadh Province (276 patients). We retrieved their

medical records from endoscopy unit database and internal medicine clinics database to extract data including demographic characteristics, personal medical history, and prognostic factors related to HP including diabetes and hypertension. The study period is from 2011- 2015.

**Data analysis:** Data were analyzed using statistical software Package of Social Science (SPSS 20 for windows evaluation version). In addition,  $\chi^2$  tests were used for categorical variables and the Mann-Whitney U test for continuous variables;  $P < .05$  is considered statistically significant.

**Data management and confidentiality:** Data identified initially and then coded in the database excel sheet using a unique identification number. The data stored on a password-protected laptop with PI; and all data maintained confidential. The publication only presented summary statistics and no identifying information is used.

## Results

Over the five years period of the study, overall, a total of 276 confirmed cases of HP were recorded on monthly basis. Figure 1 shows the monthly prevalence of HP during each months of the five years' period. Thus, the month of January, February etc. show total number of recorded HP cases in all January, February etc. falling in the five years' study time. The figure shows on an average, most number of cases diagnosed during the first five calendar months, starting from January until May ranging from 24 to 38 cases respectively. The maximum number was observed in May (38 cases). However, in June and July the Prevalence of infection dropped drastically to as low as 12 and 6 respectively. Subsequently, from August until December the Prevalence of HP increased slightly (ranging from 13 to 24) as shown in Figure 1.

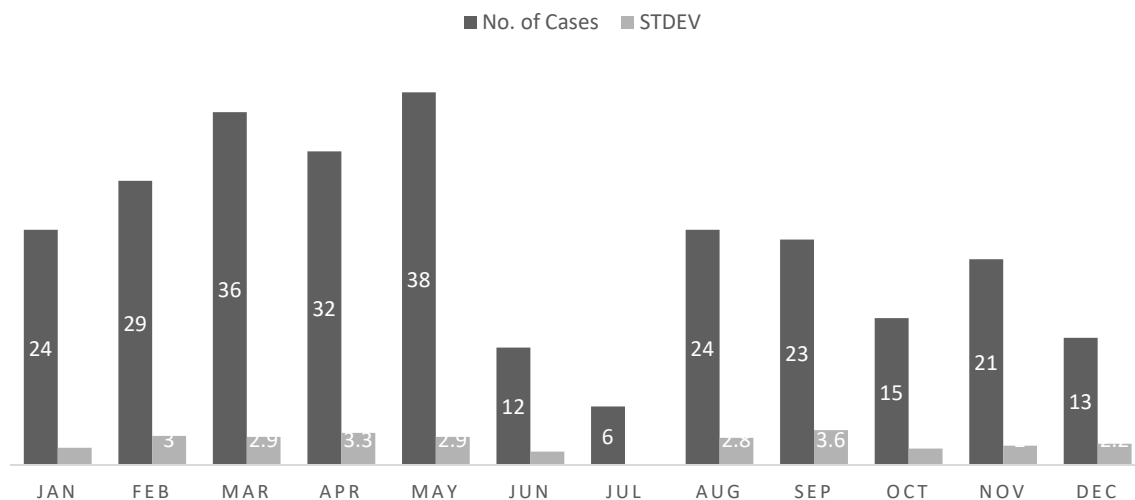


**Figure 1: Incidence of *H. pylori* infections over the 12 calendar months during the entire 5 years' observation period.**

**Table 1: Occurrence of *H. pylori* cases with other chronic diseases concurrently.**

Chronic Disease + <i>H. Pylori</i>	No of Cases
(Diabetes Mellitus (DM	20
(Hypertension (HTN	19
Anemia	5
(Peptic ulcer disease (PUD	4
(Gall bladder stone (G.B. stone	4
Hypothyroidism	3
(.Atrial fibrillation (A.F	2
(.Chronic Renal Failure (C.R.F	2
(.Benign Prostatic Hypertrophy (B.P.H	2
Brucellosis	1
(Gastro esophageal reflux disease (GERD	1
(.Bronchial asthma (B.A	1
(.Ischemic Heart Disease (I.H.D	1
Thyroiditis	1
Anorexia	1

**Table (2): Age distribution among patients with diabetes mellitus (DM) & *H. pylori* infection concurrently**

Age group in years	Total HP cases	No. of Patients with HP + DM	Percentage of patients with DM + HP
1 – 14 yrs	02	0	0.0%
15 – 39 yrs	160	3	1.9%
40 – 64 yrs	84	10	11.9%
≥ 65	30	7	23.3%
<b>Total</b>	276	20	37.1%

The prevalence of HP infections was higher in the age group between 15-39 years old. The distribution of HP infections cases was 2, 160, 84 and 30 for the age groups 0-4, 5-14, 15-39 and 40-64 and ≥ 65 years old respectively.

Different chronic diseases in addition to HP if and when were observed in the patient's files were also recorded. As shown in Table1, out of the 276 confirmed cases with HP, the patients were also suffering from some chronic diseases. The main diseases included

diabetes and hypertension (number of cases 20 and 19 respectively) with other chronic diseases but at low incidence ranging from 1 to 5 cases (Table 1).

Although most of the HP cases (56%) were observed in the age group (15-39 years) of the total cases (Table 2), it is difficult to link this age group with the HP prevalence, due to the fact that this group is already contributing to the half population of the Kingdom of Saudi Arabia. Therefore, it is expected that higher number of cases would be fall in this group. However, the results show gradual increase in concurrent occurrence of HP and diabetes cases with the age factor. The percentage of patients having both diseases was 23.3%, 11.9%, 1.9% and 0% corresponding to the age groups  $\geq 65$ , 40-64, 15-39, and 1-14 years respectively.

Similar to the data observed for HPI and diabetes are observed with hypertension as shown in Table 3. However, 30% of patients  $\geq 65$  years old were found to suffer from hypertension, comparing to 23.3% who suffer from diabetes among the same age group.

## Discussion

This retrospective descriptive study revealed that over the five years between December 2010 and September 2015, the average annual visitors to KKH in Majmaah is around 75,000. There were at least 276 HP confirmed cases. Earlier published investigations have found that HP Infection increases with age.<sup>(20)</sup> Whereas different pattern was found here where the second age group (15-39 years old) registered the highest cases. This difference might be attributed, at least partially, to the fact that the majority of the Saudi population is under 40 years old, according to the General Authority for Statistics in the kingdom of Saudi Arabia. The age group between 15-39 years old is contributing to 45% of the total population.

Association between HP infections and different chronic diseases was investigated in many earlier published studies where patients had chronic diseases concurrently when they were diagnosed for HP infection<sup>(21, 22)</sup>. The most associated chronic diseases with HP infection cases were diabetes and hypertension with 20 and 19

**Table (3): Age distribution among patients with hypertension (HTN) & H. pylori infection concurrently**

Age group	Total HP cases	No. of Patients with HP + HTN	Percentage of patients with HTN + HP
yrs 14 – 1	02	0	0.0%
yrs 39 – 15	160	3	1.9%
yrs 64 – 40	84	7	8.3%
65 $\leq$	30	9	30%
<b>Total</b>	276	19	40.2%

cases respectively. He et al., (2014) reviewed the association between HP infection and Diabetes and they found a strong relationship between HP infection and the incidence of type 2 diabetes mellitus (T2DM), formerly known as non-insulin-dependent diabetes mellitus or adult-onset diabetes.<sup>(22)</sup>

Many evidences suggest that HP infection is associated with diabetes, and may cause insulin resistance and chronic inflammation that contribute to the disease<sup>(30)</sup>. HP -induced gastritis can potentially affect the secretion of gastric-related hormones and inflammatory cytokines<sup>(27,28)</sup>. Relation between HPI and DM is complex and goes both directions where one diseases lead to the other one. However, further studies are warranted to define the relationship between HP infection and diabetes in more details, and to characterize the mechanisms of action <sup>(22)</sup>.

On the other hand, hypertension was the second highest chronic disease to be associated concurrently with the diagnosed HP cases here with 19 patients. A significant increase in HP cases in hypertensive patients as compared to normotensives individuals has been observed. The importance of this association of HP infection with hypertension is highlighted by the possibility of an effective intervention against HP infection as the organism can be easily eradicated using simple & reliable drug regimen. However, association between HP and hypertension doesn't necessarily mean causation. <sup>(23)</sup> The association needs further investigation from prospective studies.

### Conflict of Interests

The author declares that there is no conflict of interests regarding the publication of this paper.

### Acknowledgment:

The author extends his appreciation to the Deanship of Scientific Research at Majmaah University for funding this study. Sincere gratitude to Dr. Malik Al-Ehisnawi who allowed the author to conduct the study on KKH, Mr. Bandr Alharbi for his help to retrieve required data, Prof. Mazen Qato, Prof. Shamweel Yousuf, and Mr. Kamal Shaker for their comments on an earlier versions of the manuscript. Finally, thanks to Dr. Mohammad Gazar for assistance with statistical analysis.

### References:

1. Brown LM. Helicobacter pylori: epidemiology and routes of transmission. *Epidemiol Rev.* 2000;22(2):283-97.
2. Schistosomes, liver flukes and Helicobacter pylori. IARC Working Group on the Evaluation of Carcinogenic Risks to Humans. Lyon, 7-14 June 1994. IARC Monogr Eval Carcinog Risks Hum. 1994;61:1-241.
3. Malaty HM. Epidemiology of Helicobacter pylori infection. *Best Pract Res Clin Gastroenterol.* 2007;21(2):205-14.
4. Cutler AF, Havstad S, Ma CK, Blaser MJ, Perez-Perez GI, Schubert TT. Accuracy of invasive and noninvasive tests to diagnose Helicobacter pylori infection. *Gastroenterology.* 1995;109(1):136-41.

5. Prinz C, Schwendy S, Volland P. H pylori and gastric cancer: shifting the global burden. *World J Gastroenterol.* 2006;12(34):5458-64.
6. Windle HJ, Kelleher D, Crabtree JE. Childhood *Helicobacter pylori* infection and growth impairment in developing countries: a vicious cycle? *Pediatrics.* 2007;119(3):e754-9.
7. Olmos JA, Rios H, Higa R. Prevalence of *Helicobacter pylori* infection in Argentina: results of a nationwide epidemiologic study. Argentinean Hp Epidemiologic Study Group. *J Clin Gastroenterol.* 2000;31(1):33-7.
8. Newton R, Ziegler JL, Casabonne D, Carpenter L, Gold BD, Owens M, et al. *Helicobacter pylori* and cancer among adults in Uganda. *Infect Agent Cancer.* 2006;1:5.
9. Kruszon-Moran D, McQuillan GM. Seroprevalence of six infectious diseases among adults in the United States by race/ethnicity: data from the third national health and nutrition examination survey, 1988--94. *Adv Data.* 2005(352):1-9.
10. Thjodleifsson B, Asbjornsdottir H, Sigurjonsdottir RB, Gislason D, Olafsson I, Cook E, et al. Seroprevalence of *Helicobacter pylori* and cagA antibodies in Iceland, Estonia and Sweden. *Scand J Infect Dis.* 2007;39(8):683-9.
11. Rupnow MF, Shachter RD, Owens DK, Parsonnet J. A dynamic transmission model for predicting trends in *Helicobacter pylori* and associated diseases in the United States. *Emerg Infect Dis.* 2000;6(3):228-37.
12. Graham DY, Shiotani A. The time to eradicate gastric cancer is now. *Gut.* 2005;54(6):735-8.
13. Yim JY, Kim N, Choi SH, Kim YS, Cho KR, Kim SS, et al. Seroprevalence of *Helicobacter pylori* in South Korea. *Helicobacter.* 2007;12(4):333-40.
14. Malaty HM, Kim JG, Kim SD, Graham DY. Prevalence of *Helicobacter pylori* infection in Korean children: inverse relation to socioeconomic status despite a uniformly high prevalence in adults. *Am J Epidemiol.* 1996;143(3):257-62.
15. Aguemon BD, Struelens MJ, Massougbodji A, Ouendo EM. Prevalence and risk-factors for *Helicobacter pylori* infection in urban and rural Beninese populations. *Clin Microbiol Infect.* 2005;11(8):611-7.
16. Ito LS, Oba-Shinjo SM, Shinjo SK, Uno M, Marie SK, Hamajima N. Community-based familial study of *Helicobacter pylori* infection among healthy Japanese Brazilians. *Gastric Cancer.* 2006;9(3):208-16.
17. Albaker WI. *Helicobacter pylori* Infection and its Relationship to Metabolic Syndrome: Is it a Myth or Fact? *Saudi Journal of Gastroenterology : Official Journal of the Saudi Gastroenterology Association.* 2011;17(3):165-9.
18. Malfertheiner P, Megraud F, O'Morain C, Bazzoli F, El-Omar E, Graham D, et al. Current concepts in the management of *Helicobacter pylori* infection: the Maastricht III Consensus Report. *Gut.*

- 2007;56(6):772-81.
19. Ayoola AE, Ageely HM, Gadour MO, Pathak VP. Prevalence of Helicobacter pylori infection among patients with dyspepsia in South-Western Saudi Arabia. Saudi Med J. 2004;25(10):1433-8.
  20. Hunt RH, Xiao SD, Megraud F, Leon-Barua R, Bazzoli F, van der Merwe S, et al. Helicobacter pylori in developing countries. World Gastroenterology Organisation Global Guideline. J Gastrointest Liver Dis. 2011;20(3):299-304.
  21. Delitala AP, Pes GM, Malaty HM, Pisanu G, Delitala G, Dore MP. Implication of Cytotoxic Helicobacter pylori Infection in Autoimmune Diabetes. J Diabetes Res. 2016;2016:7347065.
  22. He C, Yang Z, Lu NH. Helicobacter pylori infection and diabetes: is it a myth or fact? World J Gastroenterol. 2014;20(16):4607-17.
  23. MS VS, Kutty A, Annamalai N. Helicobacter pylori infection and hypertension: Is there an association? Biomed Res- India 2012;23(4):537-9.

**ORIGINAL ARTICLE**

**Comparative study of morphology, elemental constitution and crystal structure of two large sialoliths: by way of scanning electron microscope energy dispersive x-ray (EDS) and x-ray diffraction (XRD) analysis**

Bindu Das. R, M.D.S , PGDHM<sup>1</sup>, Deepti Simon, M.D.S, D.N.B, PDF<sup>2</sup> , C.R.Sobhana, M.D.S (endo), M.D.S(omfs),MOSRCS(edin)<sup>3</sup>, Akhilesh A.V, M.D.S, PGCOI, PGCE<sup>4</sup>,

1. Assistant Professor, Department of Oral and Maxillofacial Surgery, Government Dental College, Thiruvananthapuram, Kerala. India
2. Associate Professor, Department of Oral and Maxillofacial Surgery, Government Dental College, Thiruvananthapuram, Kerala.India.
3. Professor and Head, Department of Oral and Maxillofacial Surgery, Government Dental College, Thiruvananthapuram, Kerala, India.
- 4 Assistant Professor, Department of Oral and Maxillofacial Surgery, Government Dental College, Kozhikode, Kerala. India.

*Received on: 30th June, 2016; Accepted on: 10th July,2016*

*Corresponding Author*

*Dr.Bindu Das.R*

*Assistant professor, Department of Oral and Maxillo Facial Surgery,  
Government Dental College, Thiruvananthapuram , Kerala, India*

*Pin code- 695011*

*Telephone numbers: 009847013235*

*Fax number : +914952356781*

*E-mail : bindudasr@yahoo.co.in*

**Abstract**

**Aim:** The purpose of this study was to compare the morphology, elemental constitution and crystal structure of two sialoliths; one from the parotid and the other from the submandibular gland. Also to search for the evidence to suggest the epithelial or bacterial core for the initiation of sialolith.

**Materials and Methods:** Sialoliths surgically removed from ducts of parotid and submandibular glands respectively were analyzed with Scanning Electron Microscopy (SEM) and X-ray Diffractometry (XRD).

**Results and Conclusions:** Scanning Electron Microscopy (SEM) and X-ray Diffractometry (XRD) showed that the crystal structure of both sialolith were apatitic in nature. The parotid stone was composed mainly of calcium phosphate, while its submandibular component incorporated calcium carbonate as well. The

**الملخص**

الهدف: هدفت هذه الدراسة الى مقارنة الشكل الظاهري والبناء العنصري والشكل المجهرى لأثنين من الحصاوي أحدهما من الغدة النكفية والأخرى من الغدة تحت الفك السفلي.

منهج البحث: تم ازالة الحصوات جراحيا من قنوات الغدة النكفية والغدة تحت الفك السفلي وتم تحليلها باستخدام المجهر الالكتروني والأشعة السينية.

النتائج: أوضح كل من المجهر الالكتروني والأشعة السينية أن الشكلالمجهرى للحصوتين هما من الفوسفيت في الطبيعة. الحصوة المستخرجة من الغدة النكفية تتكون بصفة اساسية من فوسفات الصوديوم بينما تحتوي حصوة الغدة تحت الفك

content of carbon also varied between the two large sialolith. The presence or absence of microorganisms could not be determined conclusively from the present study. Thus in accordance with these study results, it may be concluded that sialoliths in the salivary glands may arise secondary to sialadenitis, but not via an organic nidus.

Key words: large sialolith, scanning electron microscopy, x-ray diffractometry

السفلي كربونات الكالسيوم ايضا. يختلف مكون الكربون بين الحصوتين. وجود أحياء دقيقة لا يمكن تحديده من هذه الدراسة.

الخلاصة: تخلص الدراسة الى أن الحصوات التي تحدث بالغدد اللعابية قد تنتج بطريقة ثانوية من التهاب الغدد اللعابية وليس من مصدر عضوي.

## Introduction

Sialolithiasis is a disorder of salivary glands characterised by formation of calculi; resulting from deposition of calcium salts inside the salivary duct or gland proper. It comprises more than 50% of major salivary gland disorders and is a common reason for salivary gland infections<sup>[1]</sup>. Many theories have been stipulated to explain salivary calculi formation, such as calcification around foreign bodies, desquamated epithelial cells, and microorganisms in the duct<sup>[2,3]</sup>. Sialoliths have an organic matrix of carbohydrates and aminoacids; and are surrounded by calcium phosphate, with traces of magnesium and ammonia. Though the exact mechanism of sialolith formation is still a matter of conjecture; it has been traditionally thought to develop around a central nidus of mucous plugs, desquamated epithelial cells, micro organisms or any other foreign body. This nidus causes salivary stasis and accretion of calcium and phosphate onto it followed by slow crystallization<sup>[4]</sup>. Sialoliths range from 1mm to less than 1cm in size; and rarely grow larger than 1.5cms. Salivary sialoliths are predominantly composed of elements

comprising Ca, P, and small amounts of Mg, K, Na, Cl, Al, and Fe<sup>[5,6,7]</sup>. In general, sialoliths are composed of an organic and inorganic matrix, the presence of a central core, a laminar peripheral structure, and a major component of calcium phosphate<sup>[8,9,10]</sup>

This article showcases two large sialoliths, one each from the parotid and the submandibular gland. We have attempted to analyse its chemical composition and micromorphology by X-ray diffraction analysis (XRD), scanning electron microscopy (SEM) energy dispersive X-ray (EDS) respectively, in order to add evidence on the little understood mechanism of sialolith formation.

## Materials and Method

### Case-1

A 45-year-old South Indian female was examined in the outpatient department, with a swelling in the right cheek of 3 years duration. Her medical and dental histories were otherwise normal. Intraoral examination revealed a hard, ovoid swelling at the opening of the Stenson's duct. Radiographs revealed a radiopaque lesion that was removed

transorally. The sialolith was 1.84 cms long and weighed 5.03 gms (Fig 3A). Postoperative healing was uneventful and the patient was disease free 13 months after surgery.

### Case-2

A 42-year-old South Indian male presented to the outpatient department complaining of a painful swelling in the left side of the floor of the mouth of 20 years duration. His medical and dental history were otherwise unexceptional. Intraorally there was a hard, oblong swelling extending along the entire left lingual vestibule. At the posterior most limit, there was a draining sinus. A radiopaque mass was seen in the region of the Wharton's duct on the radiograph (Fig 3B). Under local anesthesia, a 4.13 cms long sialolith was dissected out transorally (Fig 3C). It weighed 11.04gms and the surface was nodular. Ten months after surgery the patient is symptom free and had a normal salivary flow.

### Method

The sialoliths were stored for 12 hours in 10% neutral buffered formalin, rinsed in distilled water and dried in air. They were then halved, one each for scanning electron microscopy and x-ray diffractometry. The samples were analysed for morphology, elemental constitution and crystal structure using Scanning electron microscope coupled with an EDS system (SEM-EDS) and X ray powder diffractometry (XRD).

Scanning Electron Microscopy (SEM)

and Energy Dispersive X ray analysis were done using a FEI- Quanta Environmental scanning electron microscope. The SEM samples were not subjected to any coating. Energy dispersive x-ray microanalysis was done with Large Field Detector (LFD) detector system. The SEM studies were examined at an accelerating voltage of 30 kV and a working distance of 11.7 mm for the inner surface of the parotid sialolith (Fig 1A). The outer surface of the parotid stone was studied at an accelerating voltage of 30 kV and a working distance of 12.1mm (Fig 1B). The inner (Fig 2A) and outer (Fig 2B) surfaces of the submandibular sialolith was examined at an accelerating voltage of 30 kV and working distance was 11.0mm and 10.9mm respectively.

For x-ray diffractometry the samples were powdered in an agate mortar. The procedure was carried out using Model D5005 Siemen, Karlsruhe, Germany using Cu K $\infty$  (Copper K alpha) radiation with scan speed of 5 degree per minute, with a step size of 0.1 degree. The scanning was done for a two theta angle of 10 to 90 degree. As the sample size was minimal no statistical analysis was possible.

### Results

SCANNING ELECTRON MICROSCOPE (SEM) analysis of parotid sialolith

The inner part of the sialolith shows fine granular morphology with distributed pores of approximately 5 $\mu$  in size (Fig 1A). The surface micrograph (Fig 1B) also

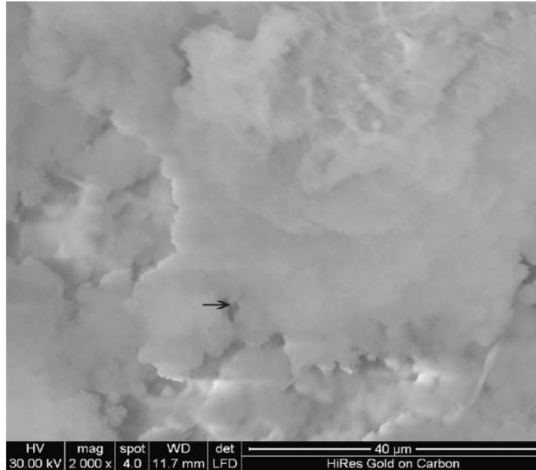


Fig. 1

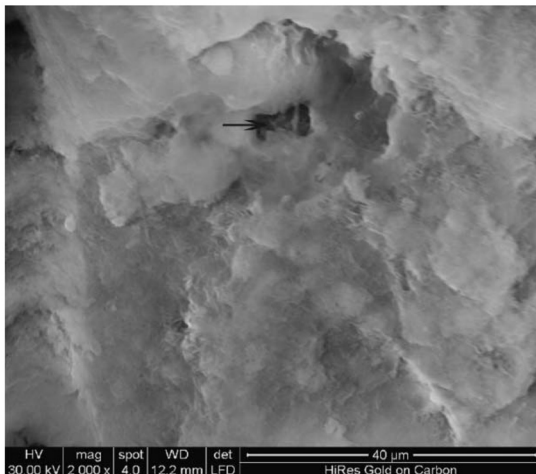


Fig. 2

shows similar microstructure. The inner part clearly shows a brittle fracture morphology emphasizing the high mineral content. The mineral content in the EDS spectra shows calcium and phosphate peaks along with oxygen and small amount of carbon. The ratio Ca/P was 1.65. This means that the mineral phase is apatitic in nature which has been further confirmed by XRD.

SCANNING ELECTRON MICROSCOPE (SEM) - Analysis of submandibular sialolith. The inner and outer surfaces of the sialolith

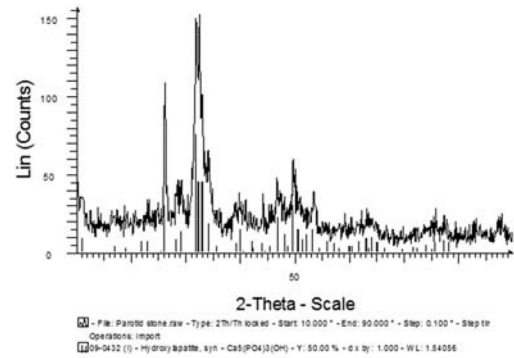


Fig. 3

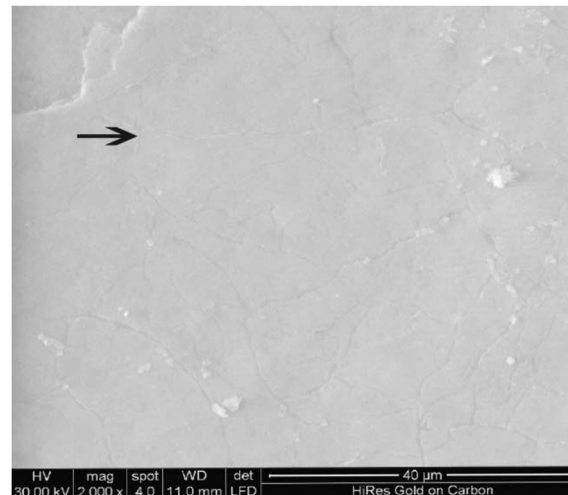


Fig. 4

show a smooth architecture (Fig 2 A, 2B) compared to the irregular morphology of the parotid sialolith. Lot of micro cracks are visible on the micrograph. EDS spectra is similar to the parotid samples in the bulk. A strong presence of carbon in the surface of submandibular samples may be due to the substitution of carbonate in the crystal structure or due to the presence of organic components like micro organisms. Further investigations are required for the confirmation.

X-RAY DIFFRACTION analyses - The XRD scan of parotid stone is Fig 1C and that of the submandibular stone is Fig 2C. Both of them are compared with the

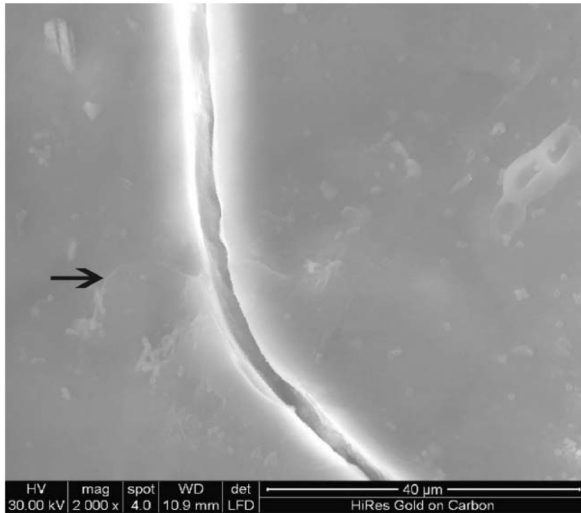


Fig. 5

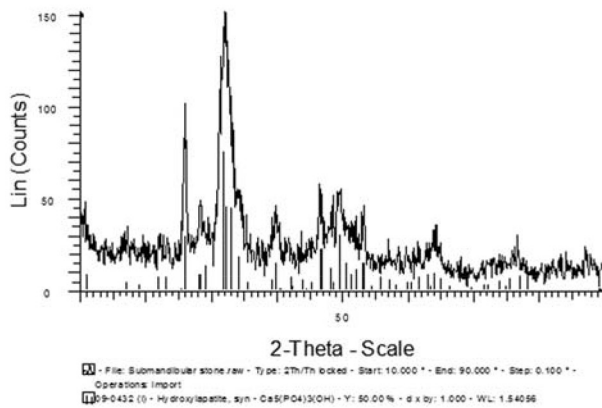


Fig. 6



Fig. 7

standard international database for synthetic hydroxyapatite PDF-9-432<sup>[22]</sup> All the peaks of the scan are matching and both the sialoliths are calcium hydroxyapatite with chemical formula  $\text{Ca}_{10}(\text{PO}_4)_6(\text{OH})_2$ . Hence it is evident that both the sialoliths are apatitic in nature. The submandibular stone shows observable amount of organic content on EDS investigation. This can be the reason of its smooth amorphous structure compared to the parotid stones.

## Discussion

Approximately 85% of sialoliths occur in the submandibular gland, 10% in the parotid, 5% in the sublingual gland and rare involvement in the minor salivary glands<sup>[11]</sup>. Males are more prone to develop salivary stones with a peak occurrence between 20 and 50 years. Submandibular stones are commonly located in the ductal system whereas parotid stones are seen in the hilum or gland parenchyma<sup>[12]</sup>. The greater predilection for sialolithiasis in the submandibular system could be due to the flow of saliva against gravity, as the Wharton's duct lies above the gland. Drage et al, postulated that the length of the duct might be of significance in the formation of submandibular stones<sup>[13]</sup>. The alkaline nature of the saliva, its viscosity, and its relatively high content of calcium salts (3.6mEq/l) compared to 2.0mEq/l of parotid are other reasons. Salivary stasis and viscosity, rather than the calcium content of saliva predispose to the development of sialoliths<sup>[14]</sup>. The submandibular saliva contains a higher

quantity of mucin protein compared with serous parotid saliva. Partial obstruction plays a greater role in the formation of stones than complete obstruction.

Salivary calculi are generally composed of an organic and inorganic matrix, a core, a laminar peripheral structure and a major component of calcium phosphate<sup>[8,9,10]</sup>. Kasaboglu et al in an ultrastructural analysis of six submandibular sialoliths, state that Ca and P are predominant on all the surfaces with traces of Na, Mg, Cl, Si, Fe and K on the internal, external and central surface matrices<sup>[15]</sup>. This may be due to the more unstable, unsaturated structure of the external and internal surfaces compared to the core. No foreign body, organic material or signs of microorganism dependent core formation were detected. Crystalloids of sialoliths are composed of either multiple and polymorphous microcrystals or a large compact crystalline mass and an occasional finding in the parotid gland<sup>[16,17]</sup>. Crystalloids present in the parotid gland may aggregate to form nuclei of calculi on which successive layers of organic and inorganic material from saliva would be deposited. Hirade and Nomura opine that a foreign body or microorganism that acts as a nucleus of initial stone formation may lose its original contour during calculi development<sup>[6]</sup>. They indicated that a foreign body or microorganism acts as a nucleus of initial stone formation and the nucleus might be morphologically changed during the calculus development so that the foreign body or microorganism eventually loses its

contour<sup>[6]</sup>. Harrison et al indicate that the stagnation of calcium rich material secondary to inflammation acts as a nucleus which later grows into a sialolith<sup>[20]</sup>. During chronic submandibular sialadenitis, inflammatory swellings would lead to the partial obstruction of a large duct with stagnation of secretory material rich in calcium. This would form a calcified core and later, when this grows, it would become a sialolith.<sup>[15]</sup> Accordingly, microorganisms have not been found in the core of the sialoliths. Since the mechanisms of calculi formation are largely speculative, all of the above theories may in part contribute to its genesis.

In the present study, the parotid stone surface was more irregular and had a higher mineral content than the submandibular counterpart. Another finding was that the parotid calculi were mainly calcium phosphate whereas the submandibular stone incorporated carbonate too. This should be further evaluated given the fact that submandibular saliva has less bicarbonate concentration than parotid (18mEq/l vs 20 mEq/l). The parotid stone had a lesser carbon content which may suggest lesser microbial content or it may be due carbonate substitution in the submandibular calculi. The higher mineral composition of parotid should also be investigated considering the organic nature of its saliva. Salivary calculi are mainly composed of calcium phosphate and carbonate and small amounts of magnesium, potassium chloride, and ammonium.<sup>[15]</sup> Likewise, the sialoliths examined in this study contained

predominantly Ca and P on all surfaces. The Ca/P ratio of parotid sialolith was 1.65 which showed the apatitic nature of the mineral phase .

The aim of this study was to analyse sialoliths using SEM and x-ray diffractometer to conduct an elemental chemical analysis on the sialoliths as well as to determine whether or not there was a foreign body or organic core causing the formation of a nucleus in the center of the sialoliths. From the findings we got with our limited methodology, the mechanism for the formation of sialoliths examined in this study was similar to the one suggested by Kasaboglu et al and Harrison et al <sup>[15, 20]</sup>

### Conclusion

Exhaustive research is necessary to elucidate the actual mechanism of evolution of sialoliths. Elemental chemical analysis should be carried out based on ageing of sialoliths to know any changes in the chemical constitution of the sialoliths as it ages.

### References

1. Escudier MP. The current status and possible future for lithotripsy of salivary calculi . Atlas Oral Maxillofac Surg Clin North Am 1998; 6: 117-132.
2. Gorlin RJ, Godman HM. Thoma's Oral Pathology. St Louis, MO, Mosby,1970, p 998.
3. Lustmann J, Shteyer A. Salivary calculi: Ultrastructural morphology and bacterial etiology. J Dent Res 1981 60:1386.
4. Bodner L. Salivary gland calculi. Diagnostic imaging and surgical management. Compend Contin Educ Dent ;1993 14:572-584.
5. Riesco JM, Juanes JA, Diaz Gonzalez MP, et al. Crystalloid architecture of a sialolith in a minor salivary gland. J Oral Pathol Med 1999; 28:451.
6. Hiriade F, Nomura Y. The fine surface structure and composition of salivary calculi. Laryngoscope 1980;90:152.
7. Mishima H, Yamamoto H, Sakae T. Scanning electron microscopy, energy dispersive spectroscopy and x-ray diffraction analyses of human salivary stones. Scanning Microsc 1992; 6:4878.
8. Ho V, Currie WJR, Walker A. Sialolithiasis of minor salivary glands. Br J Oral Maxillofac Surg 1992; 30:273
9. Isacson G, Friskopp J. The morphology of salivary calculi. A scanning electron microscopic study. Acta Odontol Scand 1984; 42:65.
10. Kodaka T, Debari K, Sano T, et al. Scanning electron microscopy and energy dispersive x-ray microanalysis studies of several human calculi containing calcium phosphate crystals. Scanning Microsc 1994; 8:241.
- 11 . Miloro M . The surgical management of submandibular gland disease. Atlas Oral Maxillofac Surg Clin North Am 1998;6:29-50.
12. Williams MF . Sialolithiasis. Otolaryngol Clin North Am 1999;32:819-834.
13. Drage NA, Wilson RF, McGurk M. The

- genu of the submandibular duct- is the angle significant in salivary gland disease, Dentomaxillofac Radiol 2002;31: 15-18.
14. Baurmash H, Dechiara SC. Extraoral parotid sialolithotomy. J Oral Maxillofac Surg 1991; 49:127- 132.
  15. Kasaboglu O, Nuray E, Tumer C, Akkocaoglu M . Micromorphology of sialoliths in the submandibular salivary gland: A Scanning Electron Microscope and X-ray Diffraction Analysis. J Oral Maxillofac Surg 2004; 62: 1253-1258.
  16. Takeda Y. Crystalloids with calcariferous deposition in the parotid gland: One of the possible causes of development of salivary calculi. J Oral Pathology 1986;15:459.
  17. Takeda Y, Ishikawa G. Crystalloids in salivary duct cysts of the human parotid gland. Scanning electron microscopical study with electron probe x-ray microanalysis. Virchows Arch 1983;399:41.
  18. Ho V, Currie WJR, Walker A. Sialolithiasis of minor salivary glands. Br J Oral Maxillofac Surg 1992; 30:273.
  19. Ademir Franco etal. Massive submandibular Sialolith:Complete radiographic registration and biochemical analysis through X-ray diffraction-a case report.case reports in surgery.vol 2014,article ID 659270.
  20. Harrison JD, Epivatianos A, Bhatia SN. Role of microliths in the etiology of chronic submandibular sialadenitis: a clinicopathological investigation of 154 cases. Histopathology.1997 ;Sep 31(3): 237-51.
  21. Szalma J etal.Proteomic and scanning electron microscopic analysis of submandibular sialoliths.Clin Oral Investig 2013 ;17(7):1709-17.
  22. Powder Diffraction File:Past,Present, and Future.Journal of Research of the National Institute of Standards and Technology.1996; 101(3).

**CASE STUDY**

## **Cystic oral lesions of salivary gland origin in children**

Case series – An Observational study

**S.Karthiga Kannan.MDS<sup>1</sup>; J. Eugenia Sherubin.MDS<sup>2</sup>; M.S. Priya MDS<sup>3</sup>,**

**Mouetaz Kheirallah Ph. D, OMFS<sup>4</sup>, Salama M.H<sup>5</sup>.**

1. Professor, Oral Medicine & Radiology,

Department of Maxillofacial surgery and Diagnostic Sciences,  
Majmaah University, Saudi Arabia.

2. Reader, Department of Oral Medicine and Radiology,

Sree Mookambika Institute of Dental Sciences, Tamilnadu state, India.

3. Consultant Prosthodontist, Sanker Ganesh Dental Hospital

Puthukkadai, KK District. Tamilnadu. India.

4. Associate Professor, Head of Department.

Department of Maxillofacial surgery and Diagnostic Sciences,  
Majmaah University, Saudi Arabia.

5. Assistant professor, College of Dentistry, Majmaah University, KSA.

Associate professor, College of Dentistry, Al-Azhar University, Egypt

Received on: 4<sup>th</sup> November, 2016; Accepted on: 19<sup>th</sup> November, 2016

Corresponding Author:

Dr.S.Karthiga Kannan.MDS

Professor, Oral Medicine & Radiology,

Department of Maxillofacial surgery and Diagnostic Sciences,

College of Dental Science,

Majmaah University,

Kingdom of Saudi Arabia.

Mobile - 00966538503869

Email- k.pillai@mu.edu.sa

### **Abstract**

Mucoceles are common benign cystic lesions of salivary gland mainly of traumatic origin. Mucoceles are known to occur most commonly on the lower lip, followed by the floor of mouth and buccal mucosa. Mucoceles are not uncommon in children.

**Objective:** To analyze the clinical characteristics of 7 mucoceles in pediatric patients who reported to us and to compare the details with the literature.

**Materials & Method:** The clinical data were retrieved from the records of 7 pediatric patients who were surgically treated for cystic lesions of minor salivary gland origin during the period of 2012 to 2015. The clinical characteristics such as gender, age, location,

### **المخلص**

تعتبر الكيُسات الفموية المخاطية أوراماً كُيسييه حميدة، غالباً ما تنشأ من الغدد اللعابية الفموية نتيجة للرضوض. تقع الكيُسات الفموية المخاطية غالباً في الغشاء المخاطي للشفة السفلية أو في قاع الفم أو الخد، والجدير بالذكر أنها نادرة الحدوث لدى الأطفال. تهدف هذه الدراسة إلى تقييم الخصائص السريرية لسبعة كيُسات مخاطية لدى مجموعة من الأطفال الذين أصيبوا بها، ثم مقارنة نتائجنا مع الدراسات العلمية السابقة. لقد تمت مراجعة السجلات الطبية واستعرضت الخصائص السريرية لسبعة كيسات نشأت من الغدد اللعابية الصغيرة وعولجت جراحياً في قسم جراحة الفم والفكين لكلية طب الأسنان بجامعة المجمعة في الأعوام ٢٠١٢-٢٠١٥ م. لقد تم تمحيص الخصائص السريرية المختلفة لتلك الحالات مثل عمر المريض، نوع وحجم ومكان

size, color, investigations and the treatment performed were evaluated and analyzed.

**Results:** This retrospective study comprised of 7 pediatric patients with mucoceles. The age ranged from 8 to 14 years. 5 were boys and 2 were girls. Four Mucoceles were located in the lower labial mucosa, two in the floor of the mouth and one in buccal mucosa. Three mucoceles measured 1.5 cms and the remaining lesions measured 1, 3, 4 and 5 cms respectively. We observed bluish hue in 3 lesions, white surface in 2, normal pink in 1 and erythematous surface in 1. On investigation 5 mucoceles showed brilliant transillumination. All mucoceles were treated with conventional surgical excision. We observed no recurrences. **Conclusion:**The observations of this study are:

1. Among the pediatric population mucoceles are commonly seen in males
2. Often detected in second decade of life.
3. The predominant site was lower labial mucosa followed by floor of the mouth.
4. The surface keratosis and internal hemorrhage can alter the characteristic bluish color.
5. Simple excision along with dissection of the affected and adjacent minor salivary gland prevents recurrence.

**Key Words** – Children, Mucocele, Ranula, Transillumination and Excision

ولون الآفة وطريقة العلاج، ثم تمت عملية التقييم والتحليل لها.

أظهرت نتائج الدراسة والتحليل بأن متوسط عمر المرضى كان ٨ إلى ١٤ عاماً فيهم خمسة ذكور وأنثيين. كان موضع الإصابة في أربعة حالات في الغشاء المخاطي للشفة السفلية، وفي حالتين في قاع الفم، وفي حالة واحدة فقط كان موقع الإصابة في الغشاء المخاطي للخد. كما تبين بأن أحجام تلك الكيسات قد تراوح بين ١-٥ سم، أما ألوانها فقد تراوحت بين الأزرق والأبيض والوردي والأحمر. عولجت جميع تلك الحالات جراحياً ولم تتعرض أي منها للنكس. ويمكن اختصار نتائج الدراسة فيما يلي:

- ١- تنتشر الكيسات المخاطية الفموية لدى الأطفال الذكور أكثر من الإناث.
  - ٢- تصيب الكيسات المخاطية الفموية مرضى العقد الثاني من العمر.
  - ٣- تقع الأكياس المخاطية الفموية غالباً في الشفة السفلية يليها قاع الفم.
  - ٤- يتغير لون الأكياس المخاطية الفموية عن اللون الأزرق الذي يميزها نتيجة النزف والتقران السطحي.
  - ٥- الاستئصال الجراحي للكيسة مع الغدة اللعابية الصغيرة يحول دون نكس الكيسة.
- الكلمات المفتاح: الأطفال، الكيسة المخاطية الفموية، الضفدعية، الاستئصال.

## Introduction

Mucocele is a soft tissue cyst of minor salivary gland origin commonly seen in the oral cavity resulting from the accumulation of saliva within the mucosa. These lesions are believed to be traumatic in origin<sup>[1]</sup>. Mucoceles can occur at any age; however some studies have reported the second decade with the highest incidence and having equal sex predilection<sup>[2]</sup>. Mucoceles are predominantly seen in lower labial mucosa followed by buccal mucosa,

ventral surface of tongue, floor of mouth and palate. The term “ranula” is positional and designates mucocele located on the floor of the mouth<sup>[3]</sup>. A rapidly progressing ranula may warrant immediate surgical attention as it may displace the tongue and threatens airway<sup>[4]</sup>. Clinically mucoceles in the labial mucosa are asymptomatic, dome shaped; smooth surfaced, soft and fluctuant. However mucoceles in the palate are superficial and resembles a vesicle or a bulla hence called as ‘*superficial mucocele*’. The color of the mucoceles may vary. When

situated deep in submucosa, it may exhibit normal pink color. Superficial lesions may exhibit characteristic bluish tint due to Tyndall effect (the diffraction of light by colloidal particles in the thick viscid mucous). As the content of the lesion is clear saliva, it allows the light to pass through and shows brilliant transillumination. Aspirations of mucocele may yield thick viscid clear mucus. Most adopted conventional treatment for mucocele is excision by scalpel or electrosurgery, which includes overlying mucosa and glandular tissue down to the muscle layer. Vaporization by carbon dioxide (CO<sub>2</sub>) laser and cryosurgery can also be done [5].



**Fig. 2a: Mucocele of 1.5 cm in size, in midline of lower lip. Aspiration showed thick mucus.**



**Fig. 2b: Excised surgical specimen under local anesthesia with associated minor salivary gland.**



**Fig. 1a: Right buccal mucosa showing a mucocele of 5cm size with bluish color.**



**Fig. 3: Lesion of 3 cm size, in left side of lower lip with mixed pink and white color.**



**Fig. 1b: Excised surgical specimen under general anesthesia.**



**Fig. 4: Ranula of 4 cm size, in the right side of floor of mouth with bluish color.**

Mucoceleles are not uncommon in children but reviews of mucoceleles in pediatric patients are extremely rare [6]. As oral health is an integral part of a child's overall health, the aim of our study is to present our data and clinical experience in the treatment of mucoceleles to increase the awareness and to remind the medical fraternity to devote much attention to lesions of the oral cavity in children.

### Materials and Method

This retrospective study included 7 pediatric patients (5 males and two females) in the age group of 8 to 14 years who were examined, diagnosed and surgically treated for cystic lesions of minor salivary gland origin in our department of oral maxillofacial surgery and diagnostic dental sciences during the period of 2012 to 2015. The Patient's clinical data on the basis of their medical records were retrieved and retrospectively investigated. The Clinical characteristics such as gender, age, location, size, color, investigations and the treatment performed were evaluated and analyzed (Table-1).

### Results

Our study comprised of 7 patients (Table - 2) with mucoceleles in the oral cavity. Among the 7 patients 5 (71%) were males and 2 (29%) were females. The age of the patients ranged from 8 to 14 years with the mean age of 11 years. Among 7 patients, 4 (57%) lesions were located in lower labial mucosa, 2

(29%) in the floor of the mouth and 1 (14%) in buccal mucosa. The size of the lesion (Table -3) varied from 1cm to 5cm with an average of 2.5cm, 3 (43%) lesions measured 1.5 cms, and the remaining lesions measured up to 1cm (14%), 2-4cm (29%) and 5cm (14%). The color of the mucoceleles varied, 3 (43%) had bluish hue, 2 (29%) were white (keratinized), 1 (14%) had normal pink color and 1 (14%) lesion was red (Table -3). While performing transillumination (Table -1) 5 (71%) lesions showed brilliant transillumination, while the 29 % lesions are white with keratotic surface and red with internal hemorrhage showed negative response. All mucoceleles were treated with conventional surgical excision and no recurrences were reported in any of the cases.

### Discussion

Mucoceleles are benign soft tissue masses resulting from the retention or extravasations of mucus in the surrounding tissues of the lamina propria. Mucus is the product of secretion of minor salivary glands [7]. The two types of mucoceleles are extravasation type and retention types [8]. The extravasation type of mucocelele arises secondary to trauma to minor salivary gland ducts resulting in the accumulation of extravasated mucous within the connective tissue of the mucosa, whereas the mucous retention type arises due to the ductal blockage either by a mucus

**Table 1. Data collection of the present study**

No	Age	Sex	Site	Size	Side	Color	Investigation	Diagnosis	Treatment	Recurrence
1	8yrs	M	Buccal Mucosa	5cm	R side	Bluish	Transillumination +Ive	Mucocele	Excision	No
2	11yrs	M	Lower Labial Mucosa	1.5cm	Midline	Bluish	Aspiration +Ive, Thick Clear Mucus	Mucocele	Excision	No
3	10	M	Lower Labial Mucosa	1.5cm	Towards L Side	Normal Pink	Transillumination +Ive	Mucocele	Excision	No
4	13yrs	M	Lower Labial Mucosa	1.5cm	Towards L Side	White - Surface Keratosis	Transillumination -Ive	Mucocele	Excision	No
5	14yrs	M	Lower Labial Mucosa	3cm	Towards L Side	White & pink Surface Keratosis	Transillumination +Ive	Mucocele	Excision	No
6	9yrs	F	Floor Of Mouth	4cm	R side	Bluish	Transillumination +Ive	Ranula	Excision	No
7	12yrs	F	Floor Of Mouth	1cm	R side	Red	Transillumination -Ive	Ranula	Excision	No

**Table 2. General characteristics of mucocele**

Age		Gender		Transillumination		Affected Site		
Groups	Number	Male	Female	Present	Absent	Buccal mucosa	Labial mucosa	Floor of mouth
I	1-5	0	0	0	0	0	0	0
II	6-10	3	1	3	0	1	1	1
III	11-15	4	1	2	2	0	3	1
Total number		7	2	5	2	1	4	2
Total %		100%	29%	71%	29%	14%	57%	29%

**Table 3. Clinical morphological features**

Age		Size					Color			
Groups	Number	Upto 1cm	1-2 cm	2-4	5 cm and above	Normal pink	Red	White	Bluish	
I	1-5	0	0	0	0	0	0	0	0	
II	6-10	3	0	1	1	1	1	0	0	2
III	11-15	4	1	2	1		0	1	2	1
	Total number	7	1	3	2	1	1	1	2	3
	Total %	100%	14%	43%	29%	14%	14%	14%	29%	43%

plug or by a sialolith, resulting in retention and accumulation of saliva within the duct. Extravasation phenomenon is more common in children as compared to retention phenomenon probably due to trauma. However Ranula can be of either mucous extravasation type or mucous retention type [8].

Mucoceleles are common oral lesions in children. In 1998, Dr Chen et al. reported that 28.6% of all biopsies from pediatric patients showed mucoceleles [9]. Our observation was in coincidence with a study conducted by Yamasoba et al wherein among 70 patients with mucoceleles they observed that 70% were below the age of 20 years [10]. This finding may have some importance in preparing these patients for surgery, as younger patients may require additional measures in terms of

anesthesia and sedation.

According to literature, most series reports an even distribution of mucoceleles between the sexes [2]. However we observed a higher incidence of mucoceleles in boys than in girls which was not in accordance with the reports of Olivera et al who observed a higher incidence of mucoceleles in girls 72.2% girls than 27.8% boys [11].

Mucoceleles are known to arise more commonly in labial mucosa [12]. Our observation was in concert with majority of researches, Yamasoba in their study observed 75% of mucoceleles in lower lip among the study population of 70 mucoceleles [10]. We observed two (29%) mucoceleles located in the floor of the mouth. These lesions acquire importance in the pediatric population because they have

to be differentiated from deeper and more serious conditions such as dermoid cyst, hemangioma and cystic hygroma.

The Literature states that clinically the mucoceles of the minor salivary glands are rarely larger than 1.5 cm and are superficial. Only the lesions arising from deeper areas such as the floor of the mouth (Ranula) is considerably larger, creating problems such as discomfort, interference with speech, mastication, and swallowing [13]. However in this study we observed that 3 mucoceles were 1.5 cm in size and also 3 lesions are larger in size with the largest mucocele to be found on the buccal mucosa measuring 5cms (Table-3).

Mucoceles are best treated by excision followed by dissection of affected minor salivary gland. Variations do exist in technique and depends on the size, location and accessibility of the lesion. Cryosurgery, laser are alternative nonsurgical methods [14]. In the present study all lesions had been treated with simple excision followed by dissection of the involved minor salivary gland to prevent recurrence.

### Conclusion

Mucoceles are a fairly common oral pathological condition in children, although not associated with significant morbidity; they can be the cause of discomfort, especially in the pediatric population. In this study we observed mucoceles are predominantly seen in boys in their second decade of life with lower

labial mucosa as the commonly involved site with the size ranging from 1 to 5cms. The color of the lesion varied from normal pink, red to blue. The surface keratosis and internal hemorrhage altered the characteristic bluish color in some of the lesions and simple excision along with dissection of affected and adjacent minor salivary glands caused no recurrences.

### Acknowledgement:

We like to thank wholeheartedly Dr. **D. Abdul Rahman bin Abdullah Atram**, Our **Dean of the Faculty of Dentistry Zulfi, Majmaah university** for the permission and all support extended for doing this work.

### References

- 1) Neville BW, Damm DD, Allen CM, Bouquot JE, editors. Oral and Maxillofacial Pathology. 3rd ed. Philadelphia: WB Saunders; 2008. 423-24
- 2) Jensen JL. Superficial mucoceles of the oral mucosa. Am J Dermatopathol 1990; 12:88-92
- 3) Quick CA and Lowell SH. Ranula and sublingual salivary glands. Arch Otolaryngol 1977; 103:397-400
- 4) Zhao Y, Jia Y, Chen X, Zhang W. Clinical review of 580 Ranulas. Oral Surg Oral Med Oral Pathol Oral Radiol Endod 2004; 98:281-287.
- 5) Huang IY, Chen CM, Kao YH, Worthington P. Treatment of mucoceles of the lower lip with carbon dioxide laser.

- J Oral Maxillofac Surg 2007; 65:855-8.
- 6) Nico MM, Park JH, Lourenço SV. Mucocele in pediatric patients: Analysis of 36 children. *Pediatr Dermatol* 2008; 25(3):308-11.
  - 7) Marcello Menta S. Nico, Jee Hee Park and Silvia Vanessa Lourenc. Mucocele in Pediatric Patients: Analysis of 36 Children. *Pediatric Dermatology* 2008; 25 (3):308–311.
  - 8) Pratik B.et al. Oral mucocele in pediatric patient: A case report and review of literature. *European journal of Dental Therapy and Research* 2014 3(3): 234-236
  - 9) Chen YK, Lin LM, Huang HC, Lin CC, Yan YH. A retrospective study of oral and maxillofacial biopsy lesions in a pediatric population from southern Taiwan. *Pediatr Dent*: 1998; 20:404 -10.
  - 10) Yamasoba T et al. Clinico statistical study of lower lip mucoceles. *J Head Neck* 1990; 12:316– 320.
  - 11) Oliveira DT, Consolaro A, Freitas FJ: Histopathological spectrum of 112 cases of mucocele. *Braz Dent J* 1993; 4:29–36.
  - 12) Harrison JD. Salivary mucoceles. *J Oral Surg OralMed Oral Pathol* 1975; 39:268–278.
  - 13) Piazzetta CM, Torres-Pereira C, Amenábar JM. Micro-marsupialization as an alternative treatment for mucocele in pediatric dentistry. *Int J Paediatr Dent* 2011; 17:1-5.
  - 14) Baurmash HD. Mucoceles and Ranulas. *J Oral MaxillofacSurg*: 2003; 61:369-78.

ORIGINAL ARTICLE

## Detection of Retinal Blood Vessels by using Gabor filter with Entropic threshold

Mohamed. I. Waly<sup>1, 2</sup>, Ahmed El-Hossiny<sup>3</sup>

1 Biomedical engineering department, Cairo higher institute for engineering, computer sciences and management, Cairo, Egypt

2 Medical equipment technology – collage of applied medical sciences, Majmaah University, Majmaah, KSA

3 Biomedical engineering department, high institute of engineering Shock academy Cairo, Egypt

Received on: 20<sup>th</sup> April, 2016; Accepted on: 25<sup>th</sup> May, 2016

Corresponding Author

Mohamed. I. Waly

email: m.waly@mu.edu.sa

### Abstract

Diabetic retinopathy is the basic reason for visual deficiency. This paper introduces a programmed strategy to identify and dispense with the blood vessels. The location of the blood vessels is the fundamental stride in the discovery of diabetic retinopathy because the blood vessels are the typical elements of the retinal picture. The location of the blood vessels can help the ophthalmologists to recognize the sicknesses prior and quicker. The blood vessels recognized and wiped out by utilizing Gobar filter on two freely accessible retinal databases which are STARE and DRIVE. The exactness of segmentation calculation is assessed quantitatively by contrasting the physically sectioned pictures and the comparing yield pictures, the Gabor filter with Entropic threshold vessel pixel segmentation by Entropic thresholding is better vessels with less false positive portion rate.

**Keywords:** Diabetic retinopathy- funds camera - Gobar filter- Entropic threshold

### الملخص

إعتلال الشبكية الذي يسببه مرض السكري هو السبب الأساسي لنقص البصر. هذا البحث يقدم استراتيجية مبرمجة لتحديد واستخلاص الأوعية الدموية داخل العين من الصور المأخوذة من قاع العين.

يعد تحديد موقع الأوعية الدموية هو خطوة أساسية في الكشف عن اعتلال الشبكية بواسطة مرض السكري لأن الأوعية الدموية هي العناصر النموذجية لصورة الشبكية. كما يمكن أن تساعد أطباء العيون بسرعة التعرف على الأمراض التي سبق ان اصابت العين.

تحديد الأوعية الدموية واستخلاصها تم باستخدام طريقة محرك الأقراص والتحديد على قاعدتي الشبكية والتي يمكن الوصول إليها بحرية عن طريق مرشح جبير.

كانت نسبة خطأ مرشح جبير بعد تعديل بعض العوامل أقل من قبل التعديل.

### I. Introduction

In the field of clinical ophthalmology, color retinal images obtained by a digital fundus camera, are broadly utilized for the detection and diagnosis of eye related diseases,

hypertension, and numerous vascular disorders. Visual impairment is perhaps the most dreaded complication that might result from diabetes. This occurs because of problems present in the retina, resulting in an ailment

known as retinopathy. Diabetic retinopathy is a disorder of the retinal vasculature. This condition sooner or later advances to some degree in almost all patients suffering from diabetes mellitus on the long term. The World Health Organization (WHO) states that the sum of adults with diabetes around the globe, would disturbingly escalate from a figure or 135 million in 1995 to a staggering 300 million in 2025 [1].

Computerized fundus picture investigation assumes a critical part in the PC supported analysis of ophthalmologic issue. A great deal of eye issue, and cardiovascular clutters, are known to relate to retinal vasculature changes. Numerous investigates has been done to investigate these connections. In any case, the clear majority of the examines depend on constrained information got utilizing manual or semi-computerized strategies because of the absence of robotized procedures in the estimation and examination of retinal vasculature. A fundus photo is a picture of the fundus taken by an ophthalmoscope, or a fundus camera. The primary pictures of the fundus were drawn by the Dutch ophthalmologist Van Trigt in 1853 [2]. An ordinary human fundus photo is appeared in Figure1. A typical human fundus photo is ruddy. Three noteworthy structures are displayed in an ordinary human eye fundus photo, the optic plate (or optic nerve head), the macula and veins. The optic plate gives off an impression of being a splendid locale in the picture, where all veins unite. Supply routes are brighter contrasting and veins. The

macula is a dull locale where few veins show. Therapeutic signs, for example, exudates, hemorrhages, pigmentation, vein variations from the norm, and cotton fleece spots can be distinguished utilizing fundus photos. Fundus photography is still the most financially savvy picture methodology clinically. It is likewise regularly utilized as a part of screening projects, where the photographs can be examined later for conclusion and be utilized to screen the advance in numerous ailments. In a screening system, where a great many fundus photos are taken, it is unthinkable for the ophthalmologists to exam each photograph, particularly in the amazingly relentless work, for example, measuring vessel width for each vessel fragment. Semi-automatic methods have already been introduced to partially relieve the problem [3]. However, it is still insufficient, particularly in screening projects and some populace investigates where typically in any event several fundus pictures are included. The estimation and division of the retinal vasculature is of principle enthusiasm for the determination and treatment of various ophthalmologic conditions [4, 5].

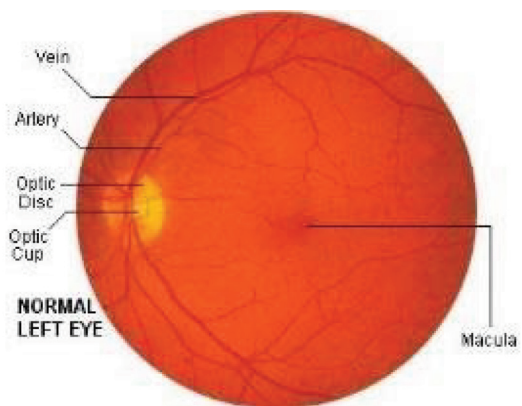


Figure1. Normal Left Eye

The exact segmentation of the retinal veins is every now and again an imperative precondition venture in the recognizable proof of retinal life systems and pathology. Moreover, the segmentation of the vessels is important for the recording of the patient pictures gained at different times [6-8]. Current vessel extraction techniques and algorithms can be categorized into four main methods as follows:

#### **a- Methods of matched filter**

Matched filtering includes convolution of the images with array of filters for extraction of objects of interest. In [9], a 2-D kernel employed to segmentation of the vasculature. The filter shape is fabricated to counterpart that of a retinal blood vessel, which typically has a Gaussian derivative or a Gaussian profile. The kernel is usually rotated in 30 to 45 degrees increments to fit into blood vessels of diverse alignments. The maximum Matched Filter Response is chosen for each pixel and is normally threshold to generate a blood vessel image. As mentioned by many authors [10-12], a Matched Filter Response technique is effective when used in integration with supplementary processing techniques. Nevertheless, the convolution kernel may be quite large and needs to be used at different rotations causing a computational overhead, which may decrease the functioning of the whole segmentation method. In addition to that, the kernel responds perfectly to blood vessels that have the same standard deviation of the underlying Gaussian equation specified

by the kernel. Thus, the kernel may not respond to blood vessels that have a dissimilar shape. The retinal low contrast of the smaller blood vessels and background variation also escalates the amount of false responses around bright objects, such as reflection artifacts and exudates. A lot of authors have suggested modifications and extensions that tackle the majority these difficulties [13-15]. In [13], the area and region based characteristics are used to detect the blood vessels in retinal fundus images. This technique observed matched filter response image using a probing technique. The probing technique classified pixels in a region of response image as vessels and non-vessels, by iteratively lessening the threshold. In each of the iteration, the probe examined the region-based attributes of the pixels in the tested region and detected the pixels classified as vessels.

#### **b- Methods of Vessel tracking**

Vessel tracking technique detect a blood vessel between two points [16-19]. Different to the formerly described techniques for blood vessels detection, they work at the level of a single blood vessel rather than the full blood vessel. The vessel tracking technique characteristically steps along the vessel. Here, the center of the longitudinal cross-section of the blood vessel is determined with different characteristics of the blood vessel including average width and tortuosity measured during tracking the blood vessel. The main benefit of vessel tracking methods lies in the fact that they offer highly accurate blood vessel

widths, and can give information about each blood vessel that is usually impossible using other methods. However, these methods required the starting point of the blood vessel, and usually the end to be located by a user, and are thus, without additional methods, of limited use in fully automated analysis. In addition, vessel-tracking methods may be confused by vessel bifurcations and crossings and often lean towards termination at branch end points.

### **c- Methods of Classifier based**

The neural networks method has been widely examined for segmenting retinal structure such as the vasculature [20]. The procedure of a neural network is equivalent to that of a matched filter. Each method takes sub windows of the image as input and returns a chance measure as output. Two different researches, each one using the back-propagation approach, have detected [21] and segmented [22, 23] the retinal vasculature. Detection involves classifying sub windows as comprising vessels or no vessels. Segmentation includes classification of each vessel and non-vessel pixels. In [22], the images are pre-processed with a principal component analysis to remove noise background. This takes place by reducing the dimensionality of the data set and then by applying a neural network to identify the pathology. They reported general specificity and affectability of 91% and 83.3%, individually. The result of the technique was contrasted and accomplished

ophthalmologist physically mapping out the area of the veins in an arbitrary example of seventy-three 20×20 pixel windows and requiring a correct match between pixels in both pictures. The neural networks researched by [21] used 20×20-pixel sub windows. Nine thousand of these sub windows were marked for neural learning validation. Generalization assessment over 1200 unseen sub windows resulted in a sensitivity of 91.7%. One of the benefits that made neural networks attractive in dividing an object into pieces of digital medical image is its capability to use nonlinear classification boundaries obtained during the training of the network and capability to learn. However, the main disadvantages of the neural networks are that they need to be trained every time whenever it is introduced to a new feature to the network, and another limitation is the necessity for constructing the network with a gold standard or training data. The gold standard data consists of several binary images whose blood vessels must be precisely segmented by a professional ophthalmologist. However, as mentioned by [13], there is an important disagreement in the empathy of the blood vessels even amongst expert observers.

### **d- Methods of Morphology**

Morphological image processing technique utilizes features of the blood vessel morphology which are called a priori, such as it being piecewise linear and connected [24-26]. Calculations that concentrate straight shapes can be exceptionally significant for

vessel division. A vessel division calculation from retinal angiography pictures in view of scientific morphology and straight preparing was offered [26]. An exceptional element of the calculation is that it utilizes a geometric model of all conceivable undesirable examples that could be gone head to head with vessels to separate vessels from them. The quality of the calculation originates from the gathering of numerical morphology and differential administrators in the division procedure. In [27], direct brilliant shapes and essential elements are removed utilizing scientific morphology administrators and vessels are extricated utilizing arch separation and Laplacian filter. Applying morphological closing to assist in recognizing of veins in the automated grading of venous beading by filling in any holes in the skeleton outline of the vein created throughout the processing method. The major disadvantage of wholly depending upon morphological methods is that they do not make use of the known blood vessel cross-sectional shape. In addition, this method works very well in the status of normal retinal images with uniform contrast, but this method works badly with noise due to diseases within the digital retinal images of eye [28].

This paper presents the blood vessels detection techniques based on Gabor filter with vessel pixel segmentation by Entropic thresholding on the fundus images because it is very fast and requires lower computing power. Therefore, the system can be used even on a very poor computer system.

## II. Material and Method

The general flow chart for the blood vessels detection shown in Figure 2.

**Stage 1:** The digital color retinal fundus images mandatory for create an automatic system are obtained from two publicly available retinal databases which are named DRIVE [29] and STARE [13].

**The STARE Database:** The images in the STARE (Structured Analysis of Retina) database comprise of twenty-one retinal fundus slides and their ground truth. The images are digitized slides captured by a Top Con TRV-50 fundus camera with 35°-degree field of view. Each slide was digitized to yield a 605 x 700-pixel image with 24bits per pixel. Figure.3 demonstrates a sample of an image present in the STARE database.

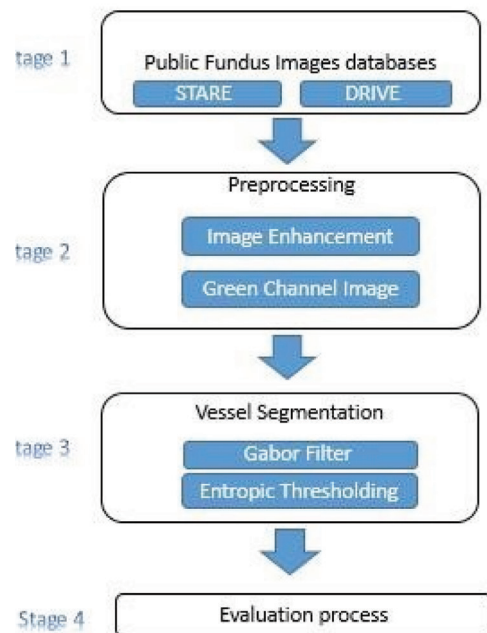


**Figure 2. General flow chart for blood vessels segmentation**

**The DRIVE Database:** The DRIVE (Digital Retinal Images for Vessel Extraction) database, which is the second image database, comprises 40 color fundus photographs and their ground truth images. All the images in the DRIVE database are digitized using a Cannon CR5 non-mydratric 3CCD camera with a 45° field of view. Each image is captured using 24-bits per pixel at the image size of 565×584. Figure.4 below shows an example of images in the database.

### Stage 2: Preprocessing

Many factors can contribute towards causing a substantial quantity of images to be of an inferior quality. Such factors range from

patient movement, poor focus, bad positioning, reflections, to inadequate illumination, as well as other similar factors, all which interfere with the analysis. Roughly 10% of the retinal images has objects that are weighty enough to obstruct human grading. Preprocessing of similar images can make certain achieve a satisfactory level in the automated detection of abnormalities. In the retinal images, there can be disparities that are instigated by numerous factors, including differences in cameras, illumination, acquisition angles, as well as retinal pigmentation. Initially during the preprocessing, the green channel of the retinal image is extracted, while subduing the other two color components, that is since



Figure 3. Retinal image from STARE database.

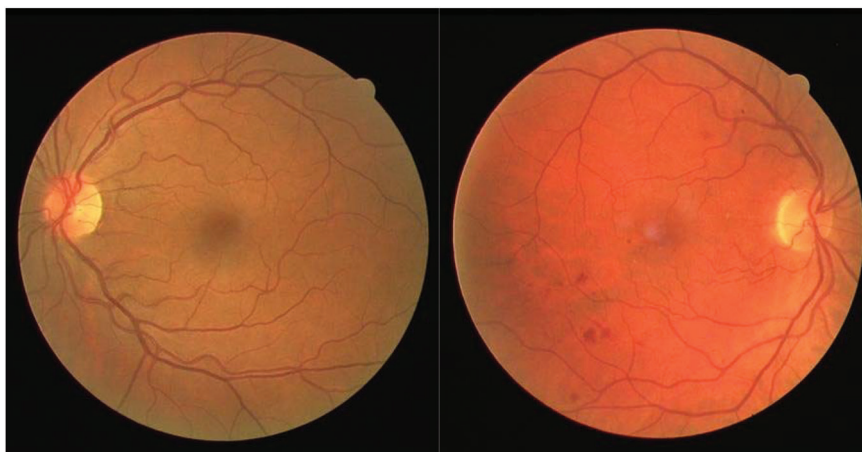


Figure 4. Retinal image from DRIVE database

most of the anatomical structure components of the retinal image appears most reliably in the green channel, as shown in figure 5. Few of the retinal images assimilated by utilizing standard clinical protocols repeatedly display low contrast. Moreover, retinal images characteristically have a higher contrast in the center of the image, with diminished contrast moving external from the center. For such images, a local contrast improvement technique is done as a second preprocessing step. Lastly, it is essential to produce a fundus mask for each image that is to enable the segmentation of lesions and anatomical structures in the following later stages. The preprocessing steps are detailed in the following subsections [30].

### Contrast Enhancement

The contrast enhancement methods are intended to modify the visual appearance,

to make an object distinct from other objects, and from the background. Typically, retinal images attained by the deployment of ordinary clinical protocols, show low contrast, and could comprise photographic items. Similarly, retinal image contrast lessened as the distance of a pixel from the center of the image escalates. In the current work, this preprocessing step is applied to the retinal images after the color normalization. Primarily, application of the histogram equalization on the intensity image produces.

It is realized that albeit the image quality is heightened, the central part of the image and the optic disc region are both over-enhanced, and this in turn causes the image to drop significant material. This is caused by histogram equalization characteristics that deals and affects the image overall. Since histogram equalization does not provide an effective structure, a Contrast-Limited

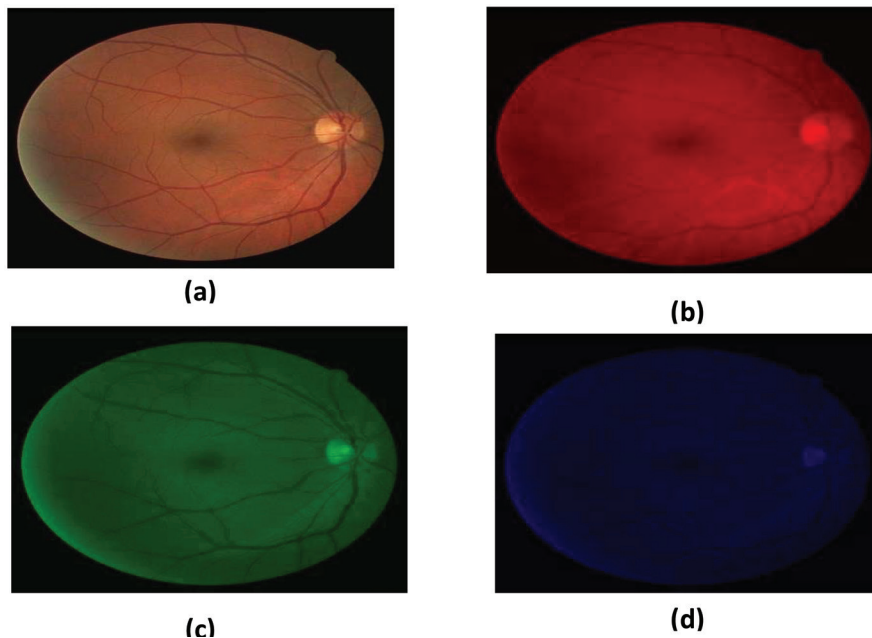


Figure 5. (a) Color retinal image; (b-d) Red, Green and image shown in figure 6.

Adaptive Histogram Equalization (CLAHE) technique was employed [22]. Whereas histogram equalization works on the whole image, CLAHE functions on small areas in the image, which called tiles. Each tile is contrast enhanced with histogram equalization. After performing the equalization, neighboring tiles are joined with the deployment of bilinear interpolation to eliminate artificially induced boundaries. While the contrast enhancement advances the contrast of exudate lesions, it also improves the contrast of some non-exudate background pixels, meaning that these pixels might be incorrectly branded as exudate lesions. For this reason, a median filtering operation is done to the intensity image prior to the contrast enhancement method, to reduce such an undesired effect [22].

**Fundus Mask Detection** The mask is a binary image, with the same resolution like that of a fundus image, whose positive pixels resemble the foreground area. It is central to distinguish between the fundus from its background, to facilitate further processing that is to be carried out only on the fundus, without interfering with those pixels belonging to the background. In a fundus mask, fundus pixels are marked as ones, while the background pixels are marked as zeros. The green channel image is threshold by a low threshold value, as the background pixels are normally considerably darker than the fundus pixels. A median filter of the size  $5 \times 5$  is deployed to eliminate any noise from the created fundus mask, and the edge pixels are eradicated by morphological erosion with

a structuring element of the size  $5 \times 5$  also. Figure 7 shows an instance of the fundus mask.

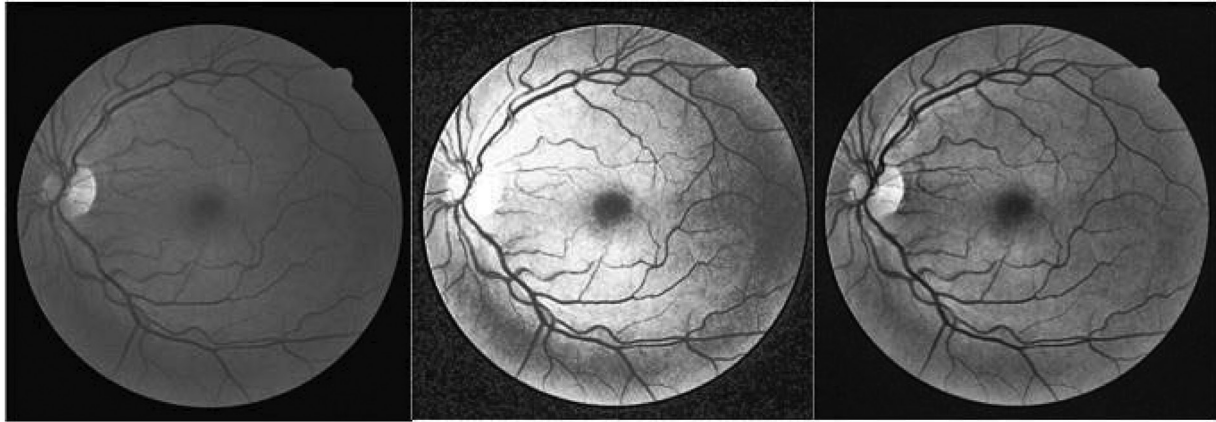
### **Stage 3: 2-D Gabor Filters for vessel enhancement.**

Gabor filters are straightforwardly connected to Gabor wavelets, as they can be designed for various dilations and rotations. Nevertheless, in general, expansion is not carried out for Gabor wavelets, due to it requiring the computation of bi-orthogonal wavelets, which might be extremely time-consuming. Consequently, more often a filter bank consisting of Gabor filters with various scales and rotations is generated. The filters involved with the signal, bringing about a so-called Gabor space. This process is thoroughly associated with processes in the primary visual cortex [31]. Jones and Palmer displayed that the real part of the complex Gabor function is a worthy fit to the receptive field weight functions found in simple cells in a cat's striate cortex [32].

The Gabor space is very helpful in image processing applications, such as optical character recognition, iris recognition, and fingerprint recognition. Associations amongst activations for a specific spatial location are very characteristic between objects in an image. Additionally, chief activations can be pulled out from the Gabor space facilitating the creation of a sparse object representation. The Gabor filters are sinusoidal modulated Gaussian functions that have ideal localization in mutually the frequency and space domains [33]. They are widely used

within the computer vision community, with special consideration to its significance to the researches of the human visual system [34]. Gabor filters have been broadly deployed to

image processing application problems, such as texture detection and segmentation [35], motion estimation, object detection, as well as strokes in character recognition [36], and



**(A)** **(B)** **(C)**  
 Figure 6. (A) Green Channel, (B) after histogram equalization, (C) after CLAHE.

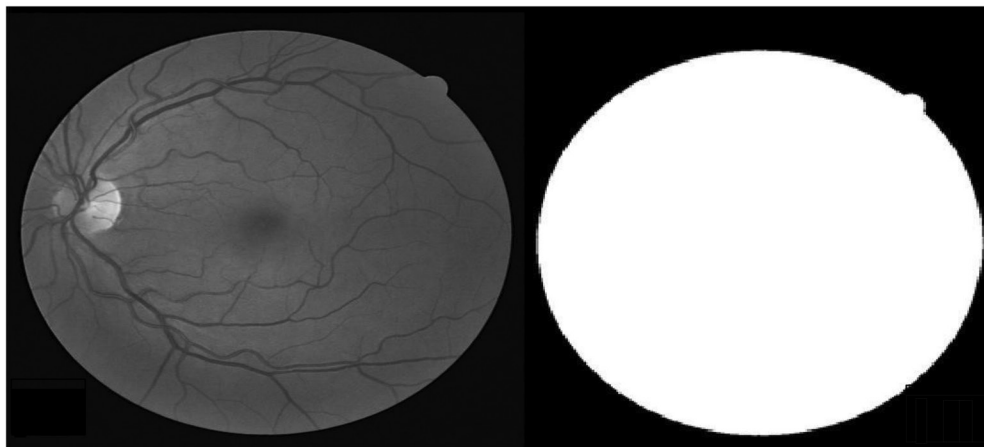


Figure 7. Automatic fundus mask generation. (a) Input image; (b) Automatically generated fundus mask.

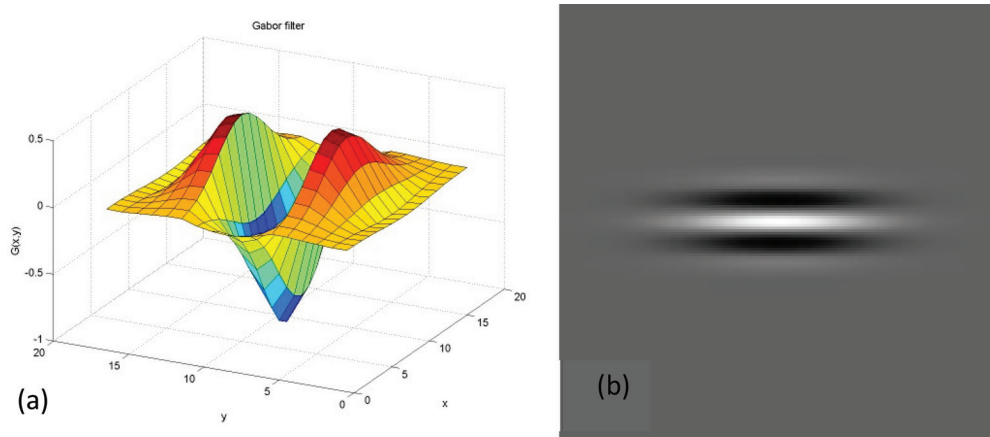


Fig. 8: Gabor filter: (a) Surface representation, (b) Real part of filter.

roads in satellite image analysis [37,38]. The three foremost properties of the Gabor filters comprise first of their ability to be tweaked to match specific orientations, which permits the drawing out of the features of line segment at any possible orientation. Secondly, the bandwidth of the filter is modifiable. Thirdly and lastly, the output of the filter is strong to noise as it uses information of all the pixels within the kernel.

The actual part of a 2D Gabor filter is utilized in the context of retinal vessel segmentation that is defined in the spatial domain  $g(x, y)$  as follows:

$$g(x, y) = \exp\left[-\pi\left(\frac{x_p^2}{\sigma_x^2} + \frac{y_p^2}{\sigma_y^2}\right)\right] \cos(2\pi f x_p) \quad (1)$$

Where,

$$x_p = x \cos \theta + y \sin \theta \quad (2)$$

$$y_p = -x \sin \theta + y \cos \theta \quad (3)$$

The parameters present in the Gabor function defined above are as follows. The angle  $\theta$  is orientation of the filter, for example, a point of zero gives a channel that reacts well to the vertical elements in a picture. The parameter  $f$  is the focal recurrence of pass band. Next,  $\sigma_x$  is the standard deviation of Gaussian in  $x$  bearing along the channel that decides the data transfer capacity of the channel. At long last,  $\sigma_y$  is the standard deviation of Gaussian over the channel that controls the introduction selectivity of the filter.

### Estimation of Gabor Parameters

The size and shape of the lines or curvilinear

structures to be identified are to be deliberated for deriving the Gabor parameters. In the case of vessel segmentation, the Gabor filter must be tweaked to a suitable frequency, so that vessels may be highlighted while background noise and other unwanted structures are filtered out. In [36], the procedure to attain the Gabor parameter values for the detection of straight line with width  $t$  has been shown. The same procedure is applied to estimate the Gabor parameters to distinguish vessels oriented in different directions.

The frequency  $f$  determines the 2D spectral centroid positions of the Gabor filter. This parameter is derived with respect to the average width of the piecewise linear segments of retinal vessels and it is set to  $f = \beta/t$  with  $\beta$  set to a proper value in the range 0.5 to 1.

$\lambda = \sqrt{2 \ln 2 / \pi}$  The standard deviation  $\sigma_x$  determines the spread of the Gabor filter in the  $\theta$  direction and it given by  $\sigma_x = \lambda t / 0.75\pi$ . The standard deviation  $\sigma_y$  that specifies the elongation of the filter is given by  $\sigma_y = 0.85 \sigma_x$ , where.

With the parameters set, the Gabor filter is thus said to be directional, as is its spatial domain, while support is in the form of an ellipse given by the elongated Gaussian of equation (1). Since, blood vessels have fluctuating diameters along diverse branches, suitable value of the thickness  $t$  must be established. When the value of  $t$  is large, most small vessels are dampened by neighboring noise. In manual segmentation, it is evident that majority of the vessel diameters are 120

$\mu\text{m}$  wide in a standard fundus image, with resolution of 20 micron/ pixels. Consequently, to provide lodging to all vessels in the image, the thickness parameter  $t$  is fixed at six, for the sake of enhancing and preserving of small vessels as well. The surface representation and real part of the resulting Gabor kernel is shown in Figure 8 with the angle  $\theta$  set to zero. It is clearly apparent that it is appropriate for the orientation of directional features to provide a good response for pixels associated with the retinal blood vessels. It is also clear that the shape of the Gabor is locally like that of a blood vessel, and this shape is maintained across different orientations. Thus, more robust Gabor responses are formed when the filter is set up at the same position, orientation and scale as a vessel in the image.

Vessel enrichment is carried out on the input retinal image to highlight the vessel structures, while at the same time suppressing the background noise and other objects. As cited previously, the green channel in the RGB image offers the finest vessel to background contrast, when compared to the red and blue channels. Hence only the green channel image is utilized for more processing in the vessel segmentation method.

Due to the directional selectivity of the Gabor filter, enhancing the pixels of vessels oriented along various directions, with the parameters described earlier, is achievable. The response of applying a Gabor filter to a vessel segment is given by:

$$r(x, y) = g(x, y) * I_g(x, y) \quad (4)$$

Where,  $g(x, y)$  is the Gabor filter defined by equation (1) and  $I_g(x, y)$  is a green channel image with vessel segment oriented along diverse directions. The shape of the filter and the vessels are alike, and that when it is situated at the center of a vessel at scale and orientation, it offers a maximum response along the vessel direction, and minimum responses along its perpendicular direction.

To identify the vessels oriented along different directions, the filter must be rotated among those directions, and only maximum response at that position is retained as follows:

$$r_{max}(x, y) = \max_{\theta} [r(x, y)] \quad (5)$$

For each pixel position in an image, spatial filtering is achieved by convolving the image with the Gabor kernel along diverse orientations. It is also found in the literature that vessel segments lying within  $\pm 7.5$  degree of the direction of the chosen kernel will respond well. So, the angle  $\theta$  of the filter is rotated from 0 to 180 degrees in steps of  $15^\circ$  to produce a single peak response on the center of a vessel segment.

### Segmentation of Vessels

When the improved retinal vessels are compared to the background, the next step is to extract the vessels from the image. To extract the enhanced vessel segments in the Gabor filter response image in an appropriate manner, an effective thresholding scheme is obligatory. The entropy based thresholding using gray level co-occurrence matrix would be applied. This technique calculates the ideal

threshold by considering the spatial spreading of the gray levels that are implanted in the co-occurrence matrix. From the co-occurrence matrix, several types of entropies such as global, local, joint and relative entropy, are computed to close the threshold value [39]. This technique is straightforward and uncomplicated to use since the co-occurrence matrix encompasses most of the information required for threshold value computation. For the appropriate segmentation of vessel pixels, a threshold is calculated using local entropy. The following section details the computation of the threshold.

#### Gray Level Co-occurrence Matrix (GLCM)

The GLCM contains information on distribute gray level frequency and edge information, as it is very useful in finding the threshold value [40, 41]. The gray level co-occurrence matrix is  $L * L$  square matrix of the gray scale image  $I$  of spatial dimension  $M * N$  with gray levels in the range  $[0, 1 \dots L - 1]$ . It denoted by  $T = [t_{i,j}]_{L*L}$  matrix. The elements of the matrix specify the number of transitions between all pairs of gray levels in a way. For each image pixel at spatial co-ordinate  $(m, n)$  with its gray level specified by  $f(m, n)$ , it considers its nearest four neighboring pixels at the locations of  $(m+1, n)$ ,  $(m-1, n)$ ,  $(m, n + 1)$  and  $(m, n - 1)$ . The co-occurrence matrix formed by comparing gray level changes of  $f(m, n)$  to its corresponding gray levels,  $f(m + 1, n)$ ,  $f(m - 1, n)$ ,  $f(m, n + 1)$  and  $f(m, n - 1)$ . Depending upon the ways in which the gray level  $I$  follows gray level  $j$ , different definitions of co-occurrence matrix

are possible. The co-occurrence matrix by considering horizontally right and vertically lower transitions is given by

$$t_{i,j} = \sum_{m=1}^M \sum_{n=1}^N \delta \quad (6)$$

Where

$$\delta = 1 \text{ if } \begin{cases} f(m, n) = i \text{ and } f(m, n + 1) = j \\ \text{or} \\ f(m, n) = i \text{ and } f(m + 1, n) = j \end{cases}$$

$$\delta = 0 \text{ otherwise}$$

Normalizing the total number of transitions in the co-occurrence matrix, a desired transition probability  $P_{i,j}$  from gray level  $I$  to gray level  $j$  is obtained as follows.

$$P_{i,j} = \frac{t_{i,j}}{\sum_{i=1}^L \sum_{j=1}^L t_{i,j}} \quad (7)$$

#### Entropic Threshold

Based on the gray level variation within or between the object and the background, the gray level co-occurrence matrix is divided into quadrants. Let  $T_h$  be the threshold within the range  $0 \leq T_h \leq -1$  that partitions the gray level co-occurrence matrix into four quadrants, namely A, B, C and D.

In the figure 9, quadrant A represents gray level transition within the object while quadrant C represents gray level transition within the background. The gray level transition is between the object and the background or across the object's boundary placed in quadrant B and quadrant D. These four regions can be further grouped into two classes, referred to as local quadrant and joint quadrant. Local quadrant refers to quadrant A and C as the gray level transition that arises within the object or the background of the

image. Then quadrant B and D are referred to as the joint quadrant because the gray level transition occurs between the object and the background of the image.

The local entropic threshold is calculated considering only quadrants A and C. The probabilities of the object class and background class are defined as:

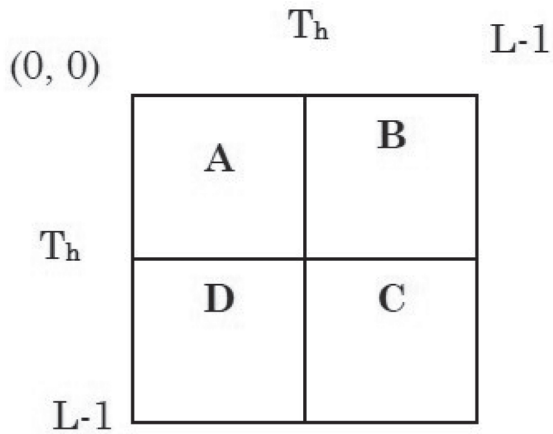


Fig. 9: Four quadrants of co-occurrence matrix.

$$P_A = \sum_{i=0}^{T_h} \sum_{j=0}^{T_h} P_{i,j} \quad (8)$$

$$P_C = \sum_{i=T_h+1}^{L-1} \sum_{j=T_h+1}^{L-1} P_{i,j} \quad (9)$$

Using equations (8) and (9) as normalization factors, the normalized probabilities of the object class and background class are functions of the threshold vector  $(T_h, T_h)$ , which is defined as:

$$P_{i,j}^A = \frac{P_{i,j}}{P_A} \quad (10)$$

$$P_{i,j}^C = \frac{P_{i,j}}{P_C} \quad (11)$$

From these, the local transition entropy A denoted by  $H_A(T_h)$  and C denoted by  $H_C(T_h)$  are calculated as follows:

The second-order entropy of the object given by:

$$H_A(T_h) = -\frac{1}{2} \sum_{i=0}^{T_h} \sum_{j=0}^{T_h} P_{i,j}^A \log_2 P_{i,j}^A \quad (12)$$

Similarly, the second-order entropy of the background given by:

$$H_C(T_h) = -\frac{1}{2} \sum_{i=T_h+1}^{L-1} \sum_{j=T_h+1}^{L-1} P_{i,j}^C \log_2 P_{i,j}^C \quad (13)$$

Both  $H(T_h)$  and  $H_C(T_h)$  are determined by the threshold  $T_h$ , thus they are functions of  $T_h$ . By summing up the local transition entropies, the total second-order local entropy of the object and the background is given by:

$$H(T_h) = H_A(T_h) + H_C(T_h) \quad (14)$$

Finally,  $T_E$ , the gray level corresponding to the maximum of  $H(T_h)$  over  $T_h$  gives the ideal threshold for the value [42]:

$$T_E = \arg \max_{T=0 \dots L-1} H(T_h) \quad (15)$$

#### Stage 4: Evaluation process

The retinal images from the DRIVE database and STARE database are used for evaluating behave the vessel segmentation method. The manually segmented vessels provided in both the databases are used as a gold standard. The entire process of segmenting vessels was carried out on a Lenovo Idea Pad Z510 laptop with i7-4700MQ (2.40GHz, 6MB) CPU and 8GB memory using MATLAB 8.3. The processing of each image including convolution and thresholding took about 18 seconds.

A bank of twelve Gabor filters, oriented in the range of 0 to 180 degrees, are used to enhance

the multi-oriented vessels. Increasing the number of filter banks did not result in significant improvement of the result, but increased the convolution operations. For each of the images, a corresponding manually segmented image is provided. Binary images with pixels are the ones determined to be part of a blood vessel by a human observer, who operated under instruct an ophthalmologist, and these images are colored white. Quantitative evaluation of the segmentation algorithm is carried out by comparing the output image with the corresponding manually segmented image. The comparison yields statistical measures that can be summarized using a contingency table, as shown in Table 1. True positives are pixels marked as vessels in both the segmentation given by a method and the manual segmentation used as ground truth. False positives are pixels marked as vessels by the method, but that are negatives in the ground truth. True negatives are pixels marked as background in both images. False negatives are pixels marked as background by

the method, but are vessel pixels.

From these, sensitivity and specificity are assessed. Sensitivity gives the percentage of pixels correctly classified as vessels by the method, while specificity gives the percentage of non-vessels pixels classified as non-vessels by the method, they are calculated as follows:

$$\text{*sensitivity*} = \frac{T_p}{T_p + F_n} \quad (16)$$

$$\text{*specificity*} = \frac{T_n}{T_n + F_p} \quad (17)$$

Where  $T_{op}$  is true positive,  $T_N$  is true negative,  $F_{op}$  is false positive and  $F_{an}$  is false negative at each pixel. The method is compared with the matched filter based method of using the DRIVE database [15].

### III. Results

An example of the quality of the obtained vessel boundary detection is shown in Figure 10 and 11. It shows a good performance on even the smallest vessels, which have low contrast. The proposed method was compared to the manual in Table 2 and Table 3.

**Table 1 Analysis using contingency table**

		Ground truth	
		Positive	Negative
Method result	Positive	(True positive ( $T_{op}$ )	(False positive( $F_{op}$ )
	Negative	(True negative( $T_N$ )	(False negative( $F_{an}$ )

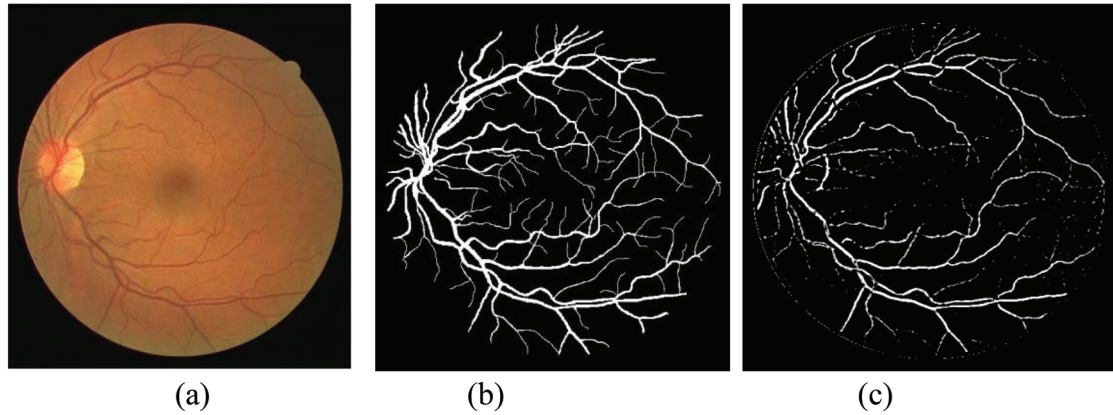


Figure 10. (a) Original image from DIRVE (b) Manual segmentation (c) the proposed approach.

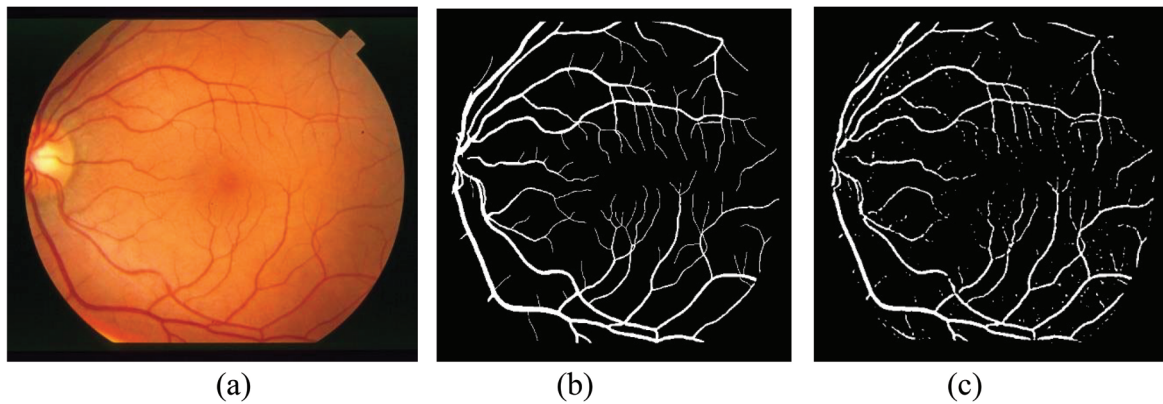


Figure 11. (a) Original image from STAR (b) Manual segmentation (c) the proposed approach

Table 2 shows that the Gabor filter is better in classifications of vessels with less false positive fraction rate.

The methods are also evaluated using the receiver operating characteristic (ROC) curve. ROC curves are formed by ordered pairs of true positive (sensitivity) and false positive (1-specificity) rates. The points on the ROC curve are attained by varying the threshold on the Gabor filter output image. For each

configuration of threshold value, a pair formed by a true positive, and a false positive rate corresponding to the method's output, is marked on the graph figure 12. The closer an ROC curve is to the upper left corner, the better is behave the method, with the point (0,1) representing a perfect agreement with the ground truth. Consequently, an ROC curve is said to dominate another if it is completely above and to the left of it. In the experiment carried out, the ideal threshold

**Table 2 retinal blood vessels segmentation method on DRIVE database.**

Method	Sensitivity (%) Mean $\pm$ SD	Specificity (%) Mean $\pm$ SD
Gabor filter	4 $\pm$ 87	2 $\pm$ 96
Matched filter	2.62 $\pm$ 83.79	3.83 $\pm$ 89.59

used to get the last output varied in steps of 5 to obtain the number of points on the ROC curve for both the methods. In Figure, it can be obviously visualized that the Gabor filter method performs better than the matched filtered based method.

The results of the proposed method are also compared with those of [13], on twenty images from the STARE database and the result is shown in Table 2. Here it is evident that the proposed method also performs better with lower specificity, even in the presence of lesions in the abnormal images.

#### IV. Conclusion

This paper highlights signify obtain an inexpensive, noninvasive, highly safe, and easy to run tool and system that will be able to streamline the procedure of screening and diagnosing of diabetic retinopathy, as carried out by the physicians, via utilizing the digital

image processing techniques to detect the main features of retinal fundus images, and some landmarks of diabetic retinopathy.

The main problems of the research were generalized the STARE database among its context, and sometimes the quality that affects directly the segmentation output. To solve this problem, we rejected 3 images from this database due to absence of several the anatomical structure, and then we applied the three image enhancement techniques to improve the quality of the images. The contrast limited adaptive histogram equalization method gave better results to advance the quality.

Ultimately, segmentations sequences executed based upon the literature review, experimental trials, and exiting packages. The segmentation stage was separated into four steps per the goal. To be able to verify the segmentation sequence, two verification

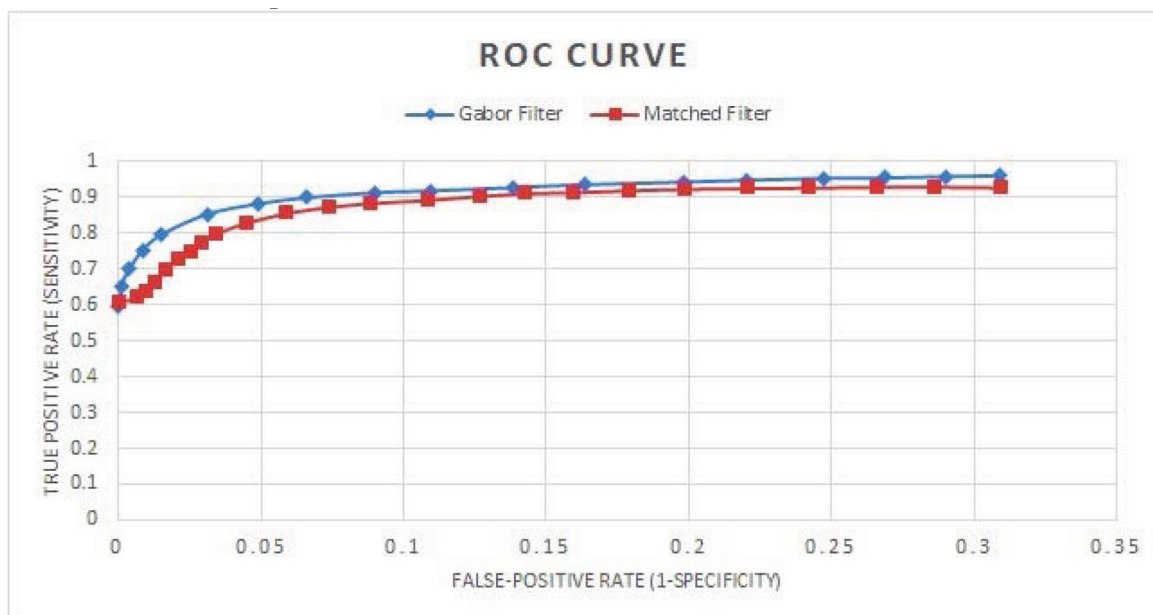


Figure 12. ROC curve of Gabor filter.

methods applied, a qualitative method as well as a quantitative method.

Gabor filters with entropic threshold have provided high-efficiency in the detection of retinal blood vessels. Large numbers of false-positive pixels observed around the optic nerve head: methods need to be developed to address this limitation. Further work is desired to design methods for ideal use of the information in the three-color components of the fundus images. The proposed methods could assist in the diagnosis of retinopathy.

### References

- 1- Siddalingaswamy, P. C., K. Gopala Krishna Prabhu, and Vikram Jain. "Automatic detection and grading of severity level in exudative maculopathy." *Biomedical Engineering: Applications, Basis and Communications* 23.03 (2011): 173-179.
- 2- Pradeepa R. Reema M., "Diabetic retinopathy: An Indian perspective," *Indian Journal of Medical Research*, vol. 125, no. 3, pp. 297-310, 2007.
- 3- Mancia, Giuseppe, et al. "2013 ESH/ESC guidelines for the management of arterial hypertension: the Task Force for the Management of Arterial Hypertension of the European Society of Hypertension (ESH) and of the European Society of Cardiology (ESC)." *Blood pressure* 22.4 (2013): 193-278.
- 4- Qutashat M., Arrar M. Al-Rawi M., "An improved matched filter for blood vessel detection of digital retinal images," *Computers in Biology & Medicine*, vol.37, no. 2, pp. 262-267, February 2007.
- 5- Johson M. J., Wiers M. Dougherty G., "Measurement of retinal vascular tortuosity and its application to retinal pathologies," *Journal of Medical & Biological Engineering & Computing*, vol. 48, no. 1, pp. 87-95, Jan 2010.
- 6- Oliveira, Francisco PM, and João Manuel RS Tavares. "Medical image registration: a review." *Computer methods in biomechanics and biomedical engineering* 17.2 (2014): 73-93.
- 7- Erlandsson, K., Buvat, I., Pretorius, P. H., Thomas, B. A., & Hutton, B. F. (2012). A review of partial volume correction techniques for emission tomography and their applications in neurology, cardiology and oncology. *Physics in medicine and biology*, 57(21), R119.
- 8- Ghassabi, Z., Shanbehzadeh, J., Sedaghat, A., & Fatemizadeh, E. (2013). An efficient approach for robust multimodal retinal image registration based on UR-SIFT features and PIIFD descriptors. *EURASIP Journal on Image and Video Processing*, 2013(1), 1-16.
- 9- Nguyen, Uyen TV, et al. "An effective retinal blood vessel segmentation method using multi-scale line detection." *Pattern recognition* 46.3 (2013): 703-715.
- 10- Aquino, Arturo, Manuel Emilio Gegúndez-Arias, and Diego Marín. "Detecting the optic disc boundary in digital fundus images using morphological, edge detection, and feature extraction techniques." *IEEE transactions on medical imaging* 29.11 (2010): 1860-1869.

- 11-Fraz, M. M., Remagnino, P., Hoppe, A., Uyyanonvara, B., Rudnicka, A. R., Owen, C. G., & Barman, S.A. (2012). Blood vessel segmentation methodologies in retinal images—a survey. *Computer methods and programs in biomedicine*, 108(1), 407-433.
- 12-Flynn J., O'Keefe M., Cahill M. Heneghan C., "Characterization of changes in blood vessel width and tortuosity in retinopathy of prematurity using image analysis," *Medical Image Analysis*, vol. 6, no. 4, pp. 407–429, 2002.
- 13-Orlando, José Ignacio, and Matthew Blaschko. "Learning fully-connected CRFs for blood vessel segmentation in retinal images." *International Conference on Medical Image Computing and Computer-Assisted Intervention*. Springer International Publishing, 2014.
- 14-Goatman, K. A., Fleming, A. D., Philip, S., Williams, G. J., Olson, J. A., & Sharp, P. F. (2011). Detection of new vessels on the optic disc using retinal photographs. *IEEE transactions on medical imaging*, 30(4), 972-979.
- 15-Zhu, Tao. "Fourier cross-sectional profile for vessel detection on retinal images." *Computerized Medical Imaging and Graphics* 34.3 (2010): 203-212.
- 16-Zhang M., Liu J. C., Bauman W. Wu D., "On the adaptive detection of blood vessels in retinal images," *IEEE Transactions on Biomedical Engineering*, vol. 53, no. 2, pp. 341-343, 2006.
- 17-Tobin, K. W., Chaum, E., Govindasamy, V. P., & Karnowski, T. P. (2007). Detection of anatomic structures in human retinal imagery. *IEEE transactions on medical imaging*, 26(12), 1729-1739.
- 18-Odstreilik, J., Kolar, R., Budai, A., Hornegger, J., Jan, J., Gazarek, J., ... & Angelopoulou, E. (2013). Retinal vessel segmentation by improved matched filtering: evaluation on a new high-resolution fundus image database. *IET Image Processing*, 7(4), 373-383.
- 19-Kaur, Jaspreet, and H. P. Sinha. "Automated detection of retinal blood vessels in diabetic retinopathy using Gabor filter." *International Journal of Computer Science and Network Security* 4.12-14 (2012): 109-116.
- 20-Kuga H. Akita K., "A computer method of understanding ocular fundus images," *Pattern Recognition*, vol. 15, no. 6, pp. 431–443, 1982.
- 21-Abràmoff, Michael D., Mona K. Garvin, and Milan Sonka. "Retinal imaging and image analysis." *IEEE reviews in biomedical engineering* 3 (2010): 169-208.
- 22-Ricci, Elisa, and Renzo Perfetti. "Retinal blood vessel segmentation using line operators and support vector classification." *IEEE transactions on medical imaging* 26.10 (2007): 1357-1365.
- 23-Leandro J. J. G., Cesar R. M, H. F. Jelinek., Cree M. J. Soares J. V. B., "Retinal vessel segmentation using the 2-D Gabor wavelet and supervised classification," *IEEE Transactions on Medical Imaging*, vol. 25,

- no. 9, pp. 1214–1222, SEP 2006.
- 24-Bernardes, Rui, Pedro Serranho, and Conceição Lobo. “Digital ocular fundus imaging: a review.” *Ophthalmologica* 226.4 (2011): 161-181.
- 25-Quellec, Gwenole, Stephen R. Russell, and Michael D. Abràmoff. “Optimal filter framework for automated, instantaneous detection of lesions in retinal images.” *IEEE Transactions on medical imaging* 30.2 (2011): 523-533.
- 26-Adal, Kedir M., et al. “Automated detection of microaneurysms using scale-adapted blob analysis and semi-supervised learning.” *Computer methods and programs in biomedicine* 114.1 (2014): 1-10.
- 27-Marín, D., Aquino, A., Gegúndez-Arias, M. E., & Bravo, J. M. (2011). A new supervised method for blood vessel segmentation in retinal images by using gray-level and moment invariants-based features. *IEEE transactions on medical imaging*, 30(1), 146-158.
- 28-Shen Z., Scott R., Kozousek V. Gregson P., “Automated grading of venous beading,” *Computers and Biomedical Research*, vol. 28, no. 4, pp. 291-304, Aug 1995.
- 29-Sommer, C., Straehle, C., Köthe, U., & Hamprecht, F. A. (2011, March). Ilastik: Interactive learning and segmentation toolkit. In *2011 IEEE international symposium on biomedical imaging: From nano to macro* (pp. 230-233). IEEE.
- 30-K. Gopalakrishna Prabhu P. C. Siddalingaswamy, “Automatic detection of multiple oriented blood vessels in retinal images,” *J. Biomedical Science and Engineering*, vol. 3, pp. 101-107, 2010.
- 31-Morel, Jean-Michel, and Sergio Solimini. *Variational methods in image segmentation: with seven image processing experiments*. Vol. 14. Springer Science & Business Media, 2012.
- 32-Niell, Cristopher M., and Michael P. Stryker. “Highly selective receptive fields in mouse visual cortex.” *The Journal of Neuroscience* 28.30 (2008): 7520-7536.
- 33-Rangayyan R. M., Frank C. B. Liu Z. Q., “Analysis of directional features in images using Gabor filters,” in IEEE, USA, 1990, pp. 68-74.
- 34-Rubinstein, Ron, Alfred M. Bruckstein, and Michael Elad. “Dictionaries for sparse representation modeling.” *Proceedings of the IEEE* 98.6 (2010): 1045-1057.
- 35-Datta, R., Joshi, D., Li, J., & Wang, J. Z. (2008). Image retrieval: Ideas, influences, and trends of the new age. *ACM Computing Surveys (CSUR)*, 40(2), 5.
- 36-MacKenzie, I. S., & Tanaka-Ishii, K. (2010). *Text entry systems: Mobility, accessibility, universality*. Morgan Kaufmann.
- 37-Tao, D., Li, X., Wu, X., & Maybank, S. J. (2007). General tensor discriminant analysis and gabor features for gait recognition. *IEEE Transactions on Pattern Analysis and Machine Intelligence*, 29(10), 1700-1715.
- 38-Liu, Laura, David Zhang, and Jane You.

- “Detecting wide lines using isotropic nonlinear filtering.” *IEEE Transactions on image processing* 16.6 (2007): 1584-1595.
- 39-Du Y., Wang J., Guo S. M., Thouin P. D. Chang C. I., “Survey and comparative analysis of entropy and relative entropy thresholding techniques,” *IEE Proceedings of Vision, Image and Signal Processing*, vol. 153, no. 6, pp. 837-850, 2006.
- 40-Gal, Y., Mehnert, A., Rose, S., & Crozier, S. (2013). Mutual information-based binarisation of multiple images of an object: an application in medical imaging. *IET computer vision*, 7(3), 1-7..
- 41-S. A. R., Abu B. Mokji M., “Adaptive thresholding based on co occurrence matrix edge information,” *Journal of Computers*, vol. 2, no. 8, pp. 44-52, 2007.
- 42-Desolneux, Agnes, Lionel Moisan, and Jean-Michel Morel. *From gestalt theory to image analysis: a probabilistic approach*. Vol. 34. Springer Science & Business Media, 2007.

ORIGINAL ARTICLE

## Convex Optimization for Energy Efficiency of a Bluetooth Based Wearable Continuous Cardiac Monitoring Node

Jaspal Singh,<sup>1</sup> , Santharaj Balakrishnan,<sup>2</sup>

<sup>1</sup> Principal Engineer, Centre for Development of Advanced Computing, Mohali – 160071 India.

Email: jaspal\_sng@yahoo.com

<sup>2</sup> Professor, Department of Medical Equipment Technology, College of Applied Medical Sciences, Majmaah University, Al

Majmaah – 11952, Kingdom of Saudi Arabia. Email: s.balakrishnan@mu.edu.sa

Received on: 20th May, 2016; Accepted on: 25th June, 2016

Corresponding Author:

Jaspal Singh

email:Jaspalsng@yahoo.com

### Abstract

Real time cardiac monitoring is an important component of body sensor networks. Due to its typical bandwidth requirements, Bluetooth is often the protocol of choice for wireless transmission from the cardiac monitoring nodes. In order to make the node small and wearable, improving energy efficiency is desirable as otherwise we end up either making the battery too big or changing it too often. In this paper we focus on optimizing energy consumption in cardiac data transmission while providing low latency. We show that this problem can be posed as a geometric program, which belongs to class of convex optimization problems. We analyse the issue based on data bandwidth requirements and latency constraints. The results are mapped to different data type specifications in Bluetooth and recommendations are drawn accordingly.

Keywords— cardiac monitoring, convex optimisation, Bluetooth, energy consumption

### الملخص

تعتبر مراقبة القلب لحظيا من العناصر الهامة في شبكات الاستشعار للجسم. و نظرا لما تحتويه تقنية البلوتوث من عرض نطاق ترددي نموذجي فانها غالبا ما تكون هي البروتوكول الأمثل للنقل اللاسلكي لمراقبة القلب من عقد المراقبة. من أجل جعل عقد المراقبة صغيرة ومن السهولة ارتداؤها، لا بد من تحسين كفاءة استخدام الطاقة بها والا ستكون البطارية كبيرة جدا أو تحتاج للتغيير كثيرا. في هذه الورقة ركزنا على تحسين استهلاك الطاقة في نقل البيانات من القلب مع توفير كمون منخفض. وقد وضحنا أن هذه المشكلة يمكن طرحها كبرنامج هندسي و الذي ينتمي إلى فئة من المشاكل المحدبة النموذجية. نحن نحلل هذه المشكلة بناء على متطلبات عرض النطاق الترددي واشكال الكمون. تم تعيين النتائج حسب أنواع البلوتوث المختلفة، ويتم رسمها التوصيات وفقا لذلك.

### I. Introduction

Real time cardiac monitoring is indicated in several healthcare scenarios. Single or multiple channel monitoring is performed in most post-operative cases. The Gold standard

for this monitoring is the use of wired monitors by the patient bedside. But wired monitoring hinders free movements of the patient and thereby, slows down the patient's recovery process also. So, a large number of researchers

have worked on / developed wireless body sensor networks (BSNs) with continuous cardiac monitoring capabilities for various scenarios [1][2][3]. These BSNs enable greater patient convenience and quicker recoveries. Apart from cardiac monitoring, wireless body sensor networks have been used for monitoring various other physiological parameters including heart rate, SpO2 levels etc. for various purposes including post-operative monitoring. Several body sensor networks and their implementations are described in the literature.[2][4][5] The applications of body sensor networks may vary widely, but continuous cardiac monitoring, remains a popular and an integral part of them.

The protocols used for wireless communications in wireless body sensor networks include Bluetooth, Bluetooth low energy, zigbee, ANT, ANT+ etc. [6]. Most of the physiological parameters like HR, PR, SpO2, RR, temperature, motion, etc. require transmission of few bytes in several seconds and thus require very little bandwidth. The parameters like ECG, EEG or EMG whenever monitored require comparatively much larger bandwidth. In such networks, often Bluetooth is the protocol of choice. [7,8,9] Bluetooth is an open standard wireless communication protocol using the 2.4GHz ISM band. It allows up to 8 connections with the master within a range of about 10-30m. The data throughput is good enough to transmit real time multichannel ECG. Recently, Bluetooth version 4.0 (referred to as Bluetooth low energy) was released as an open and license

free standard branded as ultra-low power communication.

While Bluetooth is very convenient and has suitable bandwidth for wireless cardiac monitoring, the major challenge in practical use of Bluetooth for continuous cardiac monitoring remains its energy efficiency.[10] The relatively larger data bandwidth capabilities of Bluetooth make it poorly optimized for continuous cardiac monitoring purposes. This demands use of larger battery packs which decreases the unobtrusiveness of the sensors. On the other hand, battery change / recharging is always a concern. In this paper we present a simple model of energy consumption in a wireless body sensor network and derive a cost function based on energy and latency of the data. The function is shown to belong to convex optimization problem. The simulations are then worked on the function and results are presented. The results are then discussed in the light of practical limits of bluetooth communication protocol.

## II. Network model

A wireless body sensor network may consist of several sensor nodes for measuring physiological parameters like ECG, temperature, SpO2, pulse rate, respiration rate, etc. of a subject. The nodes communicate wirelessly to a personal gateway, which could be a mobile phone, or a dedicated hardware. The hardware is often body worn, but could also be a nearby-placed node in certain scenarios. The data from the sensor nodes is continuously transferred to the gateway.

The gateway in turn transfers the data to the required destination using wires or wireless media. As most of the sensor nodes, except ECG, are comparatively less straining on the node computing resources as well as wireless resources; we focus our attention to optimisation of ECG sensing nodes. So, for the purpose of this investigation we consider network consisting of one wireless node for continuous single channel ECG monitoring. The node relays the data to a nearby placed gateway which is assumed to be sufficiently resourceful. The overview of the considered node is shown in fig 1. It has an analog front end and a microcontroller that controls sample and hold circuit, ADC and buffering. The sampling circuit continuously samples ECG signal from the amplifiers and reasonably fast ADC digitises it. The digital data is held in the buffer till the controller takes it, packetizes it and transmits to radio for further wireless transmission. Each of these steps as well as steps like generating clocks and other essential activities of controller and that of analog front end consume energy from the battery.

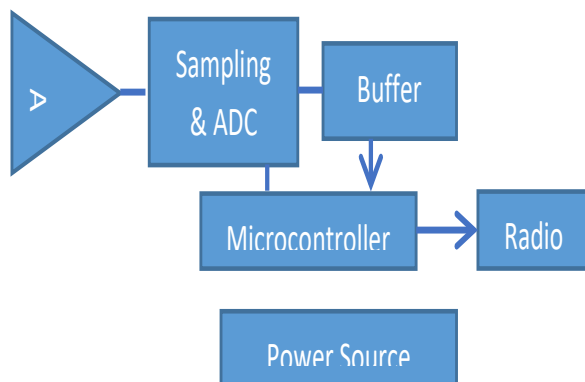


**Fig 1. The configuration of ECG Sensor Node**

We assume the radios on sensor node and gateway node work as per the Bluetooth protocol in a master - slave configuration. For simple pairing the two radios undergo a series of steps which include – device discovery, connection, security establishment and authentication before the data exchange can take place. Several of these steps can be tuned (like using dedicated bonding instead of general bonding) to improve the latency and instantaneous energy consumption [11]. However, for our purpose of continuous monitoring scenario the contribution of initial pairing and bonding exercise to the overall energy consumption is insignificant. We assume the link once established is maintained uninterrupted and the energies involved during continuous transmission are considered. The sensor node radio behaves as a master and communicates with slave in the gateway. It exchanges data packets based on the clock defined by the master. In accordance with Bluetooth classical standard, [12] each 625 microsecond interval time slot is uniquely identified and packet transmissions can begin at the start of such time interval only. The master transmits in even slots and receives in odd interval slots as shown in fig 2. A packet of transmission consists of three entities, access code, header and payload. The access code and the header have a fixed length of 72 bits and 54 bits respectively. Assuming ideal operating conditions, the payload can be anything from 0 to 2744 (or 343 bytes practically 320 bytes only) bits at the maximum.

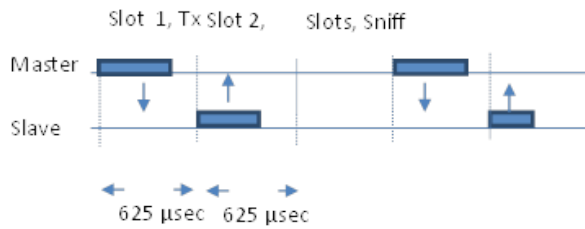


Fig 2. Indicative scheme of timing slots

### I. Optimization framework

In this section we address the problem of designing an optimal packet size and map it to convex optimization problem. We consider the case of continuous transmission of ECG data over Bluetooth link. The constraints are based on Bluetooth specifications for the radio, clinical utility of the ECG signal, buffering requirements based on packet size and the signal latency. Noting the tradeoff between energy consumption in different steps and latency, the problem of interest becomes designing optimal intervals for which the data can be buffered and then transmitted for lowest energy and latency values.

#### A. Energy consumed at the sensor node

Energy consumed at the sensor node consists of energy consumed by the radio for transmission and that consumed by other activities at the node including microcontroller activities.

Based on health condition or clinical requirements ECG requirements may vary. Let the node sample the ECG at a sampling rate 'S' per second. If the ADC is sufficiently fast, in time 't', the controller has 'S.t' digitised samples. To avoid complications, we assume contents of buffer are transmitted in a single packet. We further assume the

ADC depth of 8, so that each data sample is efficiently placed in the stream and there is no need of eliminating unwanted zeros or such manipulations anywhere in the entire system.

The radio communication is undertaken in slots of 625 μs, in compliance with Bluetooth protocol. Assuming ideal operating conditions for radio, the master node can take anything from one to five time slots of 625 μs each while one 625 μs slot is taken by the slave to acknowledge. So the radio on the node acting as master listens to slave for 625 μs, consuming 'I<sub>r</sub>' current from the battery. It then transmits using 'I<sub>t</sub>' current for one to five slots of 625 μs each. It consumes s.625.It charge during the 's' slots of transmission. Let the node go low into energy state for 'Le' time slots of 625 μs where the master radio is temporarily put in sleep mode, consuming only a sleep current of 'I<sub>s</sub>'. Assuming the complete system works at a voltage v; Energy, E consumed by the system in any time period with n different states each can be given by

$$E = v * (\sum I_n * t_n)$$

So, the energy used by radio for one transmit- receive-sleep cycle can be given by

$$E_r = v * (625.I_r + s.625.I_t + Le. 625.I_s) \quad (1)$$

This corresponds to a time, T

$$T = (1+s+Le)*625 \quad (2)$$

In this time S.(1+s+Le).625 – samples would be available and buffered. So, buffer size equal to packet payload size, P is given as

$$P = S.(1+s+Le)*625 \quad (3)$$

Total energy consumed by different operations in the controller can be estimated as sum of energies spent on analog amplification and digital processes including sampling, digitisation and buffering.

$$E_c = E_{analog} + E_{sampling} + E_{ADC} + E_{buffering} \quad (4)$$

As energy for analog amplification for any time is independent of both the sampling rate and transmission packet size, so it is ignored. Energies for sampling and ADC are considered dependent only on sampling frequency, S and do not vary with transmission packet size so, the equation 4 reduces to

$$E_c = [v * S * (I_{sa}) * T] + E_{buffering} \quad (5)$$

where,  $I_{sa}$  represents sum of currents consumed for various processes including sampling and digitisation. Using expression for sum of first n natural numbers, current for holding a buffer filling at a constant rate would be,

$$I_b * ((Peak\ buffered) * (Peak\ buffered + 1)) / 2$$

where  $I_b$  is the current consumed for buffering a sample byte. Thus,  $E_{buffering}$  comes out to be,

$$E_{buffering} = v * I_b * T * ((P) * (P + 1)) / 2 \quad (6)$$

### B. Formulation of cost function

Overall cost function is based on energy consumption and latency as the two metrics of the network performance. Energy consumption of the system is sum of energies consumed in different processes of the system. using equations 1, 5 and 6 we get the

energy E, consumed at the node as

$$E = E_c + E_r = [v * (625 * I_r + s * 625 * I_t + L_e * 625 * I_s)] + v * [S * (I_{sa}) * T] + [v * I_b * T * ((P) * (P + 1)) / 2] \quad (7)$$

Latency is defined on per sample basis as the time interval between collection of the sample and its transfer to the gateway node. Ignoring the ADC conversion time, the maximum delay in reaching of a sample is T. so the average per sample latency can be estimated as

$$L = T / 2 = (1 + s + L_e) * 625 / 2 \quad (8)$$

The overall cost function can be given as cost of energy consumption and cost of latency period.

$$C = E + \lambda * L$$

where, the E is given by equation (7) above and L is given by equation (8) above. The parameter  $\lambda$  can be interpreted as dimension equalizer. It can also be considered as relative importance given to latency with respect to energy. Combining the constraints that s can be between 1 and 5 only and that the energy given by E above is the energy based on T time periods for packet size P. Thus the optimisation problem can be written as

$$\text{Minimise } [E/P + \lambda * T/2]$$

where E is given by equation (7) above and minimization is over time period T. This is a geometric program solvable in polynomial time and thus a convex in optimisation variable T. [13].

## II. Simulation results and discussion

In order to evaluate the minimisation problem we substitute the values of different variables and vary the variables to their limits. First we consider the sampling rate. For ECG monitoring, AAMI guidelines suggest a minimum rate of 300 Hz. So,  $300 \leq S$ . A higher sampling rate would be preferable, but the simple logic that higher will increase the not only the sampling current but also the data payload and so minimum clinically advisable limit is good enough. So, we set  $S = 300$ . From the data sheets of Bluetooth module [14] we substitute  $I_r = I_t = 50\text{mA}$  and  $I_s = 20\text{mA}$  (for sniff mode or sleep mode). We vary the  $s$  from 1 to 5 for different data formats suggested in Bluetooth and summarised in table 1.

We observe ACL data type given by DH5 is most versatile and is used for getting the results. We also note that maximum latency

at the extreme of DH5 comes to be  $(794 + 6)$  slots of  $625 \mu\text{sec}$ . This comes out to be average latency of 0.25 secs, which for most practical purposes is tolerable. We set  $\lambda = 0$ . The energy curves were observed to be monotonously decreasing. The results at extreme values are tabulated in table 2.

We observe that ACL data type of DH5 is best suited for transmission of ECG signal with reasonable latency. Most Bluetooth modules which are configured for serial port profile of EDR (corresponding to payloads of 81 bytes) are actually not really the best alternative. The DH5 although apparently most suitable requires a tolerance of signal latency upto 500  $\mu\text{secs}$ . It also demands a buffer size of 150 bytes ( $=S \times \text{latency}$ ). Thus if the latency of upto 0.5 secs is allowed DH5 mode with 320 bytes of payload, 5 slots of master transmission and 794 slots of sniff mode is the optimal setting for ECG data

**Table 1. ACL Data type** <sup>[12,14]</sup>

ACL Data type	Range of variables		
	Payload (bytes) (P)	Slots of $625\mu\text{sec}$ used by master (S)	Slots of $625\mu\text{sec}$ in Sniff or sleep mode (Ts)
DH1	1 - 27	1 only	4 - 70
2-DH1 (EDR)	1-54	1 only	4-142
3-DH1 (EDR)	1-81	1 only	4-216
DH3	1-180	1-3	4-130
DH5	1-320	1-5	4-794

**Table 2. Result of simulation at extreme points**

Sample payload (bytes)	S Time slots of $625\mu\text{sec}$	Le Time slots of $625\mu\text{sec}$	Energy metric (mAs)	Average Latency msecs
1	1	4	30.0	1.875
81	1	216	22.1	68.125
320	5	794	20.2	250

transmission. The results can also be interpreted as confirmation of the fact that Bluetooth data packets have a large overhead and it is optimal to have as big payload as possible.

Also it is important to note that we have assumed ideal operating conditions and so have not accounted for ambient noise. Further, it is important to take note of the fact that we have only considered single ECG sensing node. The metrics are going to change drastically if multiple and / or heterogeneous sensors are taken into consideration of wireless body sensor network.

### III. Conclusion

We have developed a Framework for optimisation of wireless sensor node for continuous ECG transmission. The model is a geometric program which is a convex optimization problem. It can be solved for optimisation of desired parameters.

The model has been worked for standard Bluetooth data types. From the results, it is clear that making the data available to Bluetooth transmitter from the on-chip ADC is a good idea but the energy metrics are improved further if we buffer the digitised data rather than pass it straight to the radio module. Use of ACL data types DH3 or DH5 marginally improves the energy metrics of ECG sensor nodes provided noise immunity and latency are not critical. Tweaking the data transmission modes with suitable buffering to suit to DH5 can make the sensor node upto about 30% more energy efficient than transmitting signal as it becomes available.

### References

1. J. Ko, C. Lu, M. B. Srivastava, J. A. Stankovic, A. Terzis, and M. Welsh, "Wireless Sensor Networks for Healthcare," *Proceedings of IEEE*, vol. 98, no. 11, pp. 1947–1960, Nov. 2010.
2. A. K. Triantafyllidis, V. G. Koutkias, I. Chouvarda, and N. Maglaveras, "A pervasive health system integrating patient monitoring, status logging and social sharing.," *IEEE Journal of Biomed. Heal. informatics*, vol. 17, no. 1, pp. 30–7, Jan. 2013.
3. M. A. Hanson, H. C. P. Jr, A. T. Barth, K. Ringgenberg, B. H. Calhoun, J. H. Aylor, and J. Lach, "Body Area Sensor Networks :," vol. I, 2009.
4. P. Rashidi and A. Mihailidis, "A Survey on Ambient-Assisted Living Tools for Older Adults," *IEEE J. Biomed. Heal. Informatics*, vol. 17, no. 3, pp. 579–590, May 2013.
5. U. T. Pandya and U. B. Desai, "A novel algorithm for Bluetooth ECG.," *IEEE Trans. Biomed. Eng.*, vol. 59, no. 11, pp. 3148–54, Nov. 2012.
6. M. Seyedi, B. Kibret, D. T. H. Lai, and M. Faulkner, "A survey on intrabody communications for body area network applications.," *IEEE Trans. Biomed. Engineering*, vol. 60, no. 8, pp. 2067–79, Aug. 2013.
7. R. Balani, "Energy consumption analysis for bluetooth, wifi and cellular networks," [Online. <http://nesl.ee.ucla.edu/fw/documents/reports/balani.htm>, assessed

- 2nd December 2013.]
8. U. R. Shoaib, O. Rehman, Z. Akbar, and J. Iqbal, "Performance Evaluation of Bluetooth and Zigbee Using Monte Carlo Simulation," *International journal of computer science issues*, vol. 9, no. 1, pp. 235–237, 2012.
  9. H. Li and J. Tan, "Body sensor network based ECG segmentation and analysis.," *Conf. Proc. IEEE Eng. Med. Biol. Soc.*, vol. 2007, pp. 5166–9, Jan. 2007.
  10. J. Linsky, "Bluetooth and power consumption: issues and answers," *rfdesign.com*, November 2001, pp. 74–80, .
  11. T. Bourk, P. Hauser, and D. Roberts, "Simple pairing - Whitepaper" Bluetooth SIG, 2006, revision- 10r00.
  12. "Bluetooth specifications : Logical link control and adaption protocol" SIG, July 1999, pp. 247-314.
  13. Aharon Ben-Taly and Arkadi Nemirovski, "LECTURES ON MODERN CONVEX OPTIMIZATION", Georgia Institute of Technology, Fall 2013. Accessed online, <http://www.isye.gatech.edu/faculty-staff/profile.php?entry=an63> , June 2014.
  14. "Advanced user manual", Rowing networks, version 4.77, 2009.

**CASE STUDY**

**MANAGEMENT OF SIGNET-RING CELL CARCINOMA OF THE RECTUM: A CASE STUDY**

**Majed Alamri<sup>1</sup>, Helen Cecily<sup>2</sup>**

1 Assistant professor of nursing, College of Applied Medical Sciences  
Majmaah University

2 Assistant professor of nursing, College of Applied Medical Sciences  
Majmaah University

Received on: 6th November, 2016; Accepted on: 21th November, 2016

Corresponding Author:

Dr. Majed Sulaiman Alamri  
email: m.alamri@mu.edu.sa

**Abstract**

**Background:** Colorectal cancer is the third most commonly diagnosed cancer in the world. Primary signet-ring cell carcinoma of the colon and rectum (PSRCCR) is a rare form of adenocarcinoma, with a reported incidence of less than 1%. Because symptoms of PSRCCR often develop late, it usually has a poor prognosis. **Case Presentation:** A 44-year-old male presented to his general practitioner with complaints of inadequate evacuation of stool, abdominal bloating and irregular bowel movements in the last 6 months and bleeding per rectum in the past 2 weeks. Colonoscopy showed growth in the rectum; hence, a biopsy and magnetic resonance imaging (MRI) of the pelvis were done. **Discussion:** The patient received short course chemotherapy followed by low anterior resection with transverse loop colostomy. Out of 17 resected mesorectal lymph nodes, 7 nodes were positive. Due to the patient's young age and having locally advanced cancer with aggressive histology, adjuvant chemotherapy was started with intravenous (IV) oxaliplatin and oral capecitabine to prevent recurrence and improve overall survival. Patient completed 6 cycles of adjuvant therapy, after which end-to-end anastomosis was done, and the patient remained disease-free. **Conclusion:** Patients with locally advanced growth of rectal signet-ring cell carcinoma (SRCC) should be offered preoperative short-course radiotherapy

**الملخص**

خلفية: سرطان القولون والمستقيم هو ثالث أكثر أنواع السرطان تشخيصا في العالم. سرطان الخاتم الدائري للقولون والمستقيم (PSRCCR) هو شكل نادر من السرطانات الغدية، ونسبة حدوثه أقل من 1%. لأن أعراض PSRCCR غالبا ما تظهر في وقت متأخر، فإنه عادة ما يكون له مضاعفات خطيرة. عرض الحالة: شاب يبلغ من العمر 44 عاما يشتكي من الإمساك وصعوبة الإخراج، مع انتفاخ في البطن وعدم انتظام حركة الأمعاء في الستة أشهر الماضية، ونزيف في المستقيم في الأسبوعين الماضيين. أظهر فحص القولون بالمنظار نمو في المستقيم. وبالتالي، تم القيام بعمل خزعة لأخذ عينة والتصوير بالرنين المغناطيسي. المناقشة: تم إعطاء المريض جرعات من العلاج الكيميائي القصير ومن ثم اجري عملية استئصال للورم في المستقيم وتبين ان هنالك 7 نقاط إيجابية. نظرا لصغر سن المريض ووجود السرطان في مرحله متقدمة بدأ المريض العلاج الكيميائي عن طريق الفم والوريد لمنع تكرار حدوث السرطان وزيادة فرصة البقاء على قيد الحياة. اعطي المريض ستة دورات من العلاج الكيماوي بعد اجراء

with curative intent. Though the patient's cancer was in the T3N2b stage, he responded well to treatment. The chemotherapy nurse plays a significant role to ensure patients have the basic knowledge necessary to decide about treatment options.

**Key Words:** Colorectal adenocarcinoma, Signet-ring cell carcinoma, Short course radiation therapy, Adjuvant chemotherapy, Low anterior resection.

العملية الجراحية والمريض حاليا خاليا من المرض. الخلاصة: المرضى الذين يعانون من سرطان المستقيم ينبغي أن يقدم لهم علاج كيميائي قبل الجراحة. على الرغم من أن سرطان المريض في مرحلة T3n2b، فقد استجاب بشكل جيد للعلاج. ممرضة الأورام تلعب دورا هاما لضمان ان المرضى لديهم المعرفة الأساسية اللازمة لاتخاذ قرار حول خيارات العلاج.

### Introduction

Worldwide, colorectal cancer is the third most prevalent cancer in both men and women [1]. In 2012, an estimated 1.36 million new cases of colorectal cancer and 694,000 deaths were reported in the United States. In 2016, 95,270 cases of colon cancer and 39,220 cases of rectal cancer are expected to be diagnosed [2]. From 2008 to 2012, incidence rates decreased by 4.5% annually among patients older than 50 years but increased by 1.8% per year among patients younger than 50 years. Reasons for the increase in young adults, which has been consistent since at least 1992, are unknown [2].

Rectal carcinoma is broadly classified into two types: epithelial and nonepithelial tumors. Adenocarcinomas account for most of the rectal tumors in the United States [1]. One of the histologic subtypes of colorectal adenocarcinoma (CRC) is signet-ring cell carcinoma (SRCC), which has a distinct tumor biology. It is very rare to diagnose primary SRCC at an early stage as most cases are detected at an advanced stage. Therefore, overall prognosis of SRCC is poor[3].

### Case Description

**Patient History:** The subject chosen in this case study is a 44-years-old Asian male, born in India and residing in Majmaah, Saudi Arabia, when he was diagnosed with this problem. He had complaints of inadequate evacuation of stool, abdominal bloating and irregular bowel movements in the last 6 months and bleeding from the rectum in the past 2 weeks. When he developed this problem, he consulted a general practitioner in a local government hospital under the auspices of the Ministry of Health (MOH) in Saudi Arabia. Initially, he was diagnosed as having internal hemorrhoids, and was treated for the same, with no positive results. After 2 weeks, he consulted a Gastroenterologist from the same hospital. Digital rectal examination was done and the patient was advised to have a colonoscopy, after which he was diagnosed to have a growth in the rectum at 10 cm from anal verge (Fig.1). The growth was biopsied and samples sent to the pathology lab, where it a malignancy was confirmed. The then patient decided to seek further treatment at an advanced cancer center.

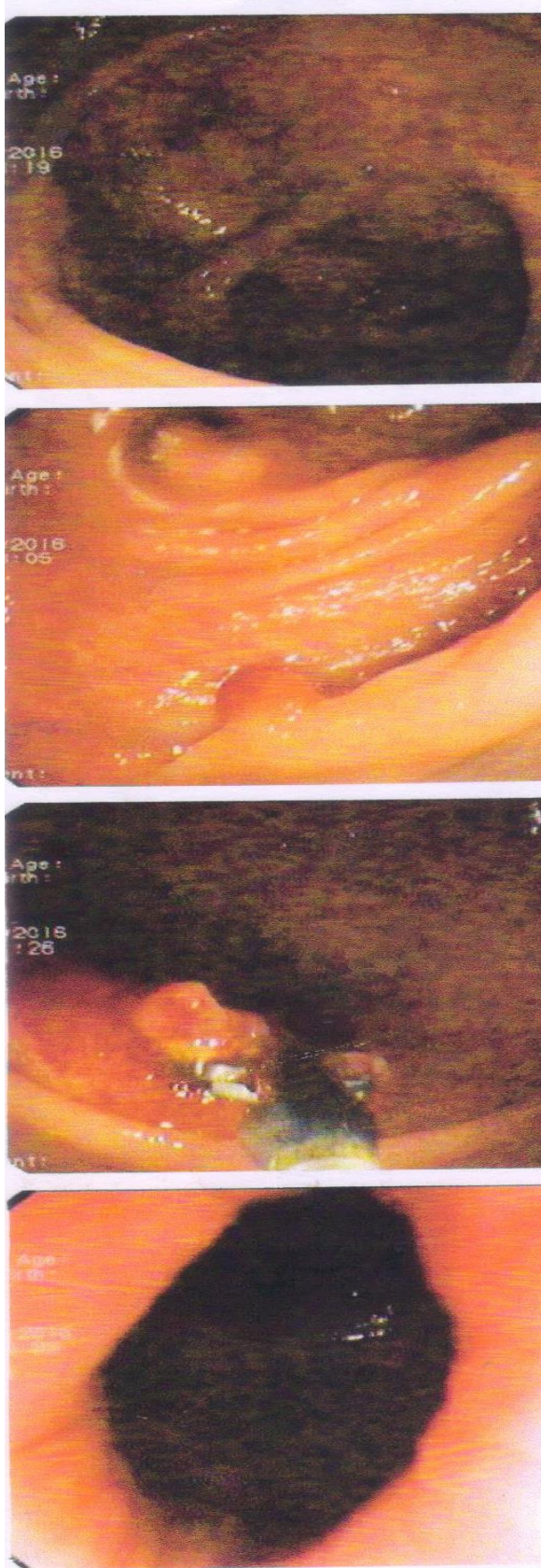


Fig. 1.

At a cancer institute, the biopsy slides and blocks were examined again in the histopathology laboratory and the results were confirmed with the same findings of signet-ring cell carcinoma. Consequently, the patient was directed to go for further blood work, including hemoglobin (Hb), total count (TC), erythrocyte sedimentation rate (ESR), differential count (DC), lipid profile, liver function test, blood carcinogenic embryonic antigen (CEA), X-ray of the chest and MRI to determine the stage of cancer. Based on the MRI result, the patient was diagnosed as having stage III rectal carcinoma mid and upper rectum T2 N0/1 M0.

#### Results of the Physical Exam:

P/A – Soft, No mass palpable, No evidence of free fluid. No inguinal nodes clinically palpable. P/R – Lower border of ulcerated growth felt at 8 cm from the anal verge, upper limit not felt.

Laboratory and Other Results: CEA – 3.2 ng/mL, Hb – 15.5 mgs/dL, WBC Total count – 6000/cumm.

Colonoscopy – Ulcerated growth at 10 cm from the anal verge, biopsies taken and small polyp at 20 cm (benign looking). Biopsy – Poorly differentiated carcinoma with signet-ring cell features. MRI Pelvis – Irregular growth involving the mid and upper rectum starting 8 cm from the anal verge. The length of the lesion is 4 cm. The lesion predominantly involves the right lateral wall with a maximum wall thickness of 1.9 cm. Minimal perirectal fat stranding noted

on right side measuring up to 5 mm with a desmoplastic reaction in the mesorectal fat. Furthermore, 2-3 tiny mesorectal nodes are seen on right side measuring up to 5 mm close to mesorectal fascia showing faint diffusion restriction. Treatment plan: The patient was given a short course of chemotherapy followed by surgery as there was not much lymph node involvement. Low anterior resection with para-abdominal colostomy and colostomy closure (end-to-end anastomosis) was planned tentatively after 12 weeks.

### **Primary Outcomes of Treatment**

Patient was treated for a 5-day period with 6Mv X-ray beam therapy using conventional technique and the total dose 20 Gy. The patient developed a mild increase in frequency of bowel elimination 3-4 times a day and burning sensation during micturition. The patient tolerated treatment well and had no other complaints.

As per the 5-day treatment plan, immediately following radiation therapy, the patient was admitted for surgery. Under general anesthesia, he underwent low anterior resection with total mesorectal excision (TME) with transverse loop colostomy (temporary colostomy). The entire tumor was removed and sent to the histopathology lab. The patient was in the recovery room for about 4 hours and then shifted to the postoperative ward. Epidural analgesia was given for about 3 days postoperatively. Also, the patient was on IV fluids and IV antibiotics, anti-emetics and H<sub>2</sub> receptor antagonists. Once the colostomy matured,

it was attached with the colostomy bag and sips of oral fluids were started gradually from the 2nd postoperative day. The patient was transferred to the postsurgical ward on the 6th postop day. Drainage tubes were removed on the 8th day postop and the abdominal wound staple pins were removed on the 9th postop day. His postoperative period was uneventful; the patient was discharged on the 10th postop day as per the plan.

It was decided to do end-to-end anastomosis after 12 weeks. Unfortunately during the surgery a locally advanced cancer was identified with the involvement of 7/17 lymph nodes. Hence, after surgery; it was determined the patient had stage T3N2b and adjuvant chemotherapy was recommended. The patient was to receive six cycles of chemotherapy with the interval of 21 days to prevent recurrence and metastasis. In each cycle, the patient received oxaliplatin 150 mg intravenously, followed by capecitabine 500 mg orally for 14 days.

### **Discussion**

Colorectal cancer is the third most commonly diagnosed cancer and the third leading cause of cancer death in the world [2]. Cancer group estimation from 2010 to 2020, shows rectal cancer as the sixth most common digestive tract cancer in India. Primary SRCC is a tumor that occurs mainly in the stomach, and less commonly in the breast, gallbladder, bladder, and pancreas [4-5]. Primary SRCC of the colon and rectum (PSRCCR) is a rare type of cancer, with a reported incidence of

less than 1%. It is frequently diagnosed at an advanced stage with positive lymph nodes and metastases because typically symptoms develop late, which results in poor prognosis [3,6,7].

Age 50 or older with a family history of cancer can affect the risk of rectal cancer. Being overweight, consuming a diet high in red meat, heavy alcohol use, smoking, and a personal history of inflammatory bowel disease are the risk factors for rectal carcinoma [4]. Signs of rectal cancer include a change in bowel habits, blood in the stool, frequent gas pains, bloating, fullness, cramps, change in appetite, weight loss for no known reason, and fatigue [1].

Furthermore, it mainly affects young adults [6,7]. Histologically, PSRCCR shows typical features that differentiate the cells from routine adenocarcinoma of the colon. The signet-ring malignant cells are seen as a cluster of isolated cells floating in abundant extracellular mucin pools [8,9].

Various modalities of treatment are available for cancer. But developing individualized treatment plans to fit each patient's distinct needs is most important. Surgery with total mesorectal excision is the treatment of choice for patients with locally advanced rectal cancer [10]. The treatment options for the patient in this case study is atypical compared to the cases reported in the literature [10-12]. Unlike other stage III rectal cancers, this patient was treated with preoperative short course radiation therapy followed by surgery, low anterior resection

with mesorectal excision. Though the patient had locally advanced rectal cancer (T3N2b), he responded well to this treatment, which is incongruent with the results of Swedish Rectal Cancer Trial conducted by Theodore and Harvey [11].

Treatment of colorectal cancer depends on its type and stage. Surgery, radiation therapy, chemotherapy and targeted therapy are the standard ways of treating this disease. Stage 0 cancer needs only excision of the tumor; stage I is treated with surgery and chemoradiation therapy if needed. Additionally, stage II and III rectal cancers are treated with surgery, preoperative chemoradiation therapy or short-course preoperative radiation therapy and postoperative chemoradiation therapy, while stage IV cancer is treated with palliative therapy [1,2].

Furthermore, patients with a clinically resectable rectum receiving short-course radiation before the operation had better local control, as well as a longer overall survival duration, than those who did not receive radiation therapy preoperatively [11].

Most colorectal cancer patients receive long course neo-adjuvant chemoradiation therapy (NACRT) before surgery to help shrink tumors, so the tumors are easily removed by surgery. Though down-staging is achieved in the majority of tumors receiving long course NACRT the extent of down-staging and survival may vary from patient to patient. Many factors in the literature predict the response to NACRT, of which advanced

stage at presentation is the most important [12]. At the same time, NACRT correlates more closely with higher acute toxicity than short-course radiation [13]. As the patient in this case study was free from acute toxicity, he was able to withstand the effects of anesthesia and surgery. Apart from his young age, various other factors such as his leukocyte count, hemoglobin level, and good general health favored the surgical outcome.

Disregarding the tumor biology and the prognosis of SRCC, 7/17 nodes were identified as positive at the time of surgery. Hence adjuvant chemotherapy that included IV oxaliplatin with oral capecitabine was initiated a month after surgery to prevent recurrence and metastasis. Oxaliplatin is a platinum-containing compound, which belongs to the large group of alkylating agents, whereas capecitabine is an antimetabolite. These drugs help ensure any cancer cells remaining after surgery are eliminated [13]. Six cycles of therapy were administered with the duration of 21 days, after which end-to-end anastomosis was done.

To date, the patient is cancer free. His prognosis was congruent with the findings of various trials [10-11]. Both studies recommend that close follow-up and intensified adjuvant therapy improves survival for patients with stage III SRCC. Postoperative adjuvant chemotherapy, which research shows results in a 25%-30% reduction in future metastases, is an accepted component of multimodal therapy [12].

### Nursing Management

Nursing care plays a vital role caring for patients with rectal carcinoma during the various modalities of treatment such as radiation therapy, surgery and postoperative chemotherapy. The patient, in this case, was prepared both physically and psychologically before these treatments. Informed consent was obtained, explaining the nature of treatments, benefits and their short-and long-term side effects.

Nursing monitored the patient for adverse effects such as skin changes, blanching, erythema, desquamation, sloughing, ulcerations of mucous membranes, nausea and vomiting, diarrhea, burning micturition or gastrointestinal bleeding, as well as white blood cell and platelet counts for significant decreases [14].

**Preliminary education:** Part of the patient's care included his and his family's education about radiation therapy and the following points:

Care of the skin at the radiation site. Instructions were specific to wash the skin marked as the radiation site with plain water only, not with soap; do not apply any deodorant or lotions, medications, perfume, or talcum powder to the site during the treatment period.

**Do not wash off the treatment marks.**

Do not rub, scratch, or scrub treated skin areas. Inspect the skin for damage or remarkable changes, and report these to the radiologist. Wear loose, soft clothing over the treated area. Protect skin from sun exposure during treatment.

Rest, drink more fluids and eat a balanced diet. Preoperative care: After the patient was cleared by a cardiologist and an anesthetist for surgery, he was admitted to the hospital 2 days before surgery. Apart from routine preoperative preparations such as lab tests, fasting, skin preparation, laxatives and enemas, the patient was given whole bowel irrigation with two liters of Peglec solution to clear the bowel. To relieve his fear and anxiety, the patient met the stoma and colostomy nurse since he would have a temporary colostomy. The patient received preoperative health teaching about postoperative wound and drainage tube care, colostomy care, dietary restrictions, and early ambulation and pain control measures (epidural analgesia), as well as education from a physiotherapist on use of the spirometer to prevent pulmonary complications postoperatively.

**Postoperative care:** After colon resection, the patient was taken to the post-anesthesia care unit and was monitored closely by the nurses till anesthesia wore off. After vital signs were stable and the patient was awake and oriented, he was transferred to the postoperative ward. The patient was on IV fluids until the colon recovered sufficiently for food and fluid to be taken by mouth. Analgesics were administered intravenously for pain management. Nothing was allowed by mouth until it was certain that normal colon function has resumed; typically the passage of stool is an indication the colon is healing. After colon function returned, the patient was given clear liquids, and the nasogastric

tube was removed. Once clear liquids were tolerated, the diet was slowly advanced until the patient was eating solid foods. The day after surgery, the patient was encouraged and assisted in moving around to stimulate bowel function and enhance blood circulation. Drainage tubes and the urinary catheter were removed on the eighth post operative day and abdominal wound staple pins were removed the next day. Postoperative period was uneventful, and the patient was discharged on the tenth post op day as per the plan.

**Nursing care during adjuvant chemotherapy:** Chemotherapy nurses ensure the patient has the basic knowledge to decide about treatment options. Accordingly, appropriate up-to-date information regarding the aim of the treatment, side effects, and outcomes were given to the patient. Clinical review and nursing assessment were done before each cycle of chemotherapy to ensure no toxicities so the patient was fit to continue. During chemotherapy, nurses assessed vein fragility to ensure there were no signs of extravasation [15].

As important as the physical assessment, is the nursing role in assessing the psychological impact of a diagnosis of cancer; and educating the patient on how to cope with chemotherapy. Body image changes such as weight loss, hair loss, skin texture, fatigue, and stoma management confound the psychological distress. Holistic needs assessment tools were used to assess the general well-being of the patient as well as the toxicities.

## CONCLUSION

Primary SRCC is a rare condition based on clinical and pathological features. This case study demonstrates exceptional management of primary SRCC of the rectum. Treatment of locally advanced primary and recurrent SRCC of the rectum with preoperative short-course radiotherapy followed by excision is associated with good prognosis. To date there is no evidence of recurrent disease in the patient. Finally, a patient with locally advanced SRCC should be offered preoperative short-course radiotherapy.

## References

1. National Cancer Institute. Rectal cancer treatment (PDQ)—Health professional version. 2016. <https://www.cancer.gov/types/colorectal/hp/rectal-treatment-pdq>
2. American Cancer Society: Cancer facts and figures 2016. <http://www.cancer.org/acs/groups/content/@research/documents/document/acspc-047079.pdf>
3. Park PY, Goldin T, Chang J, Markman M, Kundranda MN. Signet-ring cell carcinoma of the colon: A case report and review of the literature. *Case Rep Oncol* 2015;8:466-471. <https://www.karger.com/Article/Pdf/441772>.
4. American Cancer Society. Colorectal cancer. 2016. <http://www.cancer.org/cancer/colonandrectumcancer/detailedguide/colorectal-cancer-risk-factors>.
5. Kang H, O'Connell JB, Maggard MA, Sack J, Ko CY. A 10-year outcomes evaluation of mucinous and signet-ring cell carcinoma of the colon and rectum. *Dis Colon Rectum* 2005;48:1161-1168.
6. Belli S, Aytac HO, Karagulle E, Yabanoglu H, Kayaselcuk F, Yildirim S. Outcomes of surgical treatment of primary signet ring cell carcinoma of the colon and rectum: 22 cases reviewed with literature. *IntSurg* 2014;99:691-698.
7. Lee HS, Soh JS, Lee S, Bae JH, Kim KJ, Ye BD, et al. Clinical features and prognosis of resectable primary colorectal signet-ring cell carcinoma. *Intest Res* 2015; 13(4): 332-338 <http://dx.doi.org/10.5217/ir.2015.13.4.332>
8. Gopalan V, Smith RA, Ho YH, Lam AK. Signet-ring cell carcinoma of colorectum – current perspectives and molecular biology. *Int J Colorectal Dis* 2011;26:127-133
9. Ogino S1, Brahmandam M, Cantor M, Namgyal C, Kawasaki T, Kirkner G. , et al: Distinct molecular features of colorectal carcinoma with signet ring cell component and colorectal carcinoma with mucinous component. *Mod Pathol* 2006;19:59-68.
10. Glynne-Jones R, Tan D, Moran BJ, Goh V. How to select for preoperative short-course radiotherapy, while considering long-course chemoradiotherapy or immediate surgery, and who benefits? *Eur Oncol & Haematol* 2014;10(1):17-24. <http://www.touchoncology.com/articles/how-select-preoperative-short-course-radiotherapy-while-considering-long->

- course.
11. Hong TS, Mamon H. Short-course versus standard chemoradiation in T3 rectal cancer. *Oncologist* 2011 May; 16(5): 717-721. <https://www.ncbi.nlm.nih.gov/pmc/articles/PMC3228203/>.
  12. Hugen N, Verhoeven RH, Lemmens VE, van Aart CJ, Elferink MA, Radema SA, et al: Colorectal signet-ring cell carcinoma: benefit from adjuvant chemotherapy but a poor prognostic factor. *Int J Cancer* 2015;136:333-339.
  13. Hong TS Ryan DP. Adjuvant chemotherapy for locally advanced rectal cancer: Is it a given? *J Clin Oncol* 2015. <http://jco.ascopubs.org/cgi/doi/10.1200/JCO.2015.60.8554>.
  14. [http://wps.prenhall.com/wps/media/objects/737/755395/radiation\\_therapy.pdf](http://wps.prenhall.com/wps/media/objects/737/755395/radiation_therapy.pdf)
  15. Roe, H, Lennan, E. Role of nurses in the assessment and management of chemotherapy-related side effects in cancer patients. *DovePress* 2014; 4: 103-115. <https://www.dovepress.com/role-of-nurses-in-the-assessment-and-management-of-chemotherapy-relate-peer-reviewed-fulltext-article-NRR>.



## **PROPOSAL APPLICATION REQUIREMENTS AND PROCESS**

*The following are the steps in case of applying a non-funded proposal in the College of Medicine, Majmaah University, to acquire the ethical approval*

- A. **Provide the proposal in the approved format (soft)**
- **Includes signature of the principal investigator (mandatory)**
  - **Includes signature of the supervisor for student research (Mandatory)**
  - **Contact details of the principal researcher (PR)**
- B. **The proposal is sent by email to the head of the research unit (ey.mohamed@mu.edu.sa, elsadigoo@gmail.com)**
- **The proposal will be sent to the research unit members to be revised technically**
  - **Research unit holds a meeting within 7-10 days to discuss the proposal**
  - **Feedback will be conveyed to the principal researcher**
- C. **After correction by the principal researcher , if any, he/she sends the following documents to the head of the research unit:**
- **The corrected proposal**
  - **The ethical approval form**
  - **Curriculum vitae (CV) of the principal researcher**
  - **The consent form**
- **The documents will be sent to the head of the research committee to pass them to the dean then to: BASIC AND HEALTH RESEARCH CENTER ETHICAL COMMITTEE OF MAJMAAH UNIVERSITY (soft) to acquire the ethical approval**

## Mediterranean Conference for Academic Disciplines (Malta 2017)

### Conference

26th February to 2nd March 2017  
Valletta, Malta

**Website:** <http://www.internationaljournal.org/malta.html>

**Contact person:** Professor Joseph Bonnici, PhD, JD (Central Connecticut State University)

Visit the Mediterranean for a multidisciplinary conference and boat-and-bus tours of different islands. The Maltese Islands are Medieval gems. Event is hosted in 5-star hotel with affordable lodging. Submit your abstract.

**Organized by:** International Journal of Arts and Sciences  
**Deadline for abstracts/proposals: 9th January 2017**

## The 13th International Conference on Psychiatry “Controversies in Diagnosis and Treatment in Psychiatry; Professional Experiences”

### Conference

13th to 15th April 2017  
Jeddah, Saudi Arabia

**Website:** [http://jed.sghgroup.com.sa/index.php?option=com\\_content&view=article&id=324&Itemid=42&lang=en](http://jed.sghgroup.com.sa/index.php?option=com_content&view=article&id=324&Itemid=42&lang=en)

**Contact person:** Dr Mohamed Khaled

Recently there has been a growing awareness of the Controversies in Diagnosis and Treatment in Psychiatry; Professional Experiences; thus this congress will highlight these important issues.

**Organized by:** Saudi German Hospital & Saudi Psychiatric Association  
**Deadline for abstracts/proposals: 15th November 2016**

## 6th International Conference on Nanotechnology (ICN2017)

### Conference

9th to 10th February 2017  
Dubai, United Arab Emirates

**Website:** <http://icn2017.srpioneers.org>

**Contact person:** 00989902120661

6th International Conference on Nanotechnology (ICN2017), <http://icn2017.srpioneers.org> that will be in American University in Dubai on February 9-10, 2017 \*ICN2017 has been selected as one of the top ten credible conferences in the world by EUS

**Deadline for abstracts/proposals: 9th December 2016**

## 2nd World Conference on Disability and Rehabilitation 2017

### Conference

9th to 10th February 2017  
Colombo, Western, Sri Lanka

**Website:** <http://disabilityconference.co/home/>

**Contact person:** Mr Arun Francis

The Conference is believed to create a platform to address the causes for the increase in number of the disabled persons, the perception of the society towards them, their deprived rights and the solutions to overcome this global phenomenon.

**Organized by:** The International Institute of Knowledge Management

**Deadline for abstracts/proposals: 15th December 2016**

## 10th International Conference on Healthcare, Nursing and Disease Management (HNDM), 22-23 Feb 2017, Dubai

### Conference

22nd to 23rd February 2017  
Dubai, United Arab Emirates

**Website:** <http://iaphlsr.org/10th-international-conference-on-healthcare-nursing-and-disease-management-hndm-22-23-feb-2017-dubai-about-20>

**Contact person:** Dr. Pallavi R

Venue: Flora Grand Hotel, Deira, Dubai. International Publication of accepted research papers with ISSN, DOI and Indexing. Great opportunity for international Networking and Collaborations.

**Organized by:** IAPHLSR – International Association for Promotion of Healthcare and Life Science Research

**Deadline for abstracts/proposals:** 20th February 2017

## International Conference on Healthcare, Applied Science and Engineering

### Conference

17th to 18th March 2017  
Vienna, Austria

**Website:** <http://americanhealthcare.wix.com/science-vienna>

**Contact person:** Dr.Samah Khalil

These conference is for those, who are interested in presenting papers in all fields of Healthcare, Applied Science and Engineering.

**Organized by:** Ontario College for Research and Development

**Deadline for abstracts/proposals:** 10th March 2017

## 16th Annual Design of Medical Devices Conference

10th to 13th April 2017  
Minneapolis, Minnesota, United States of America

**Website:** <http://www.dmd.umn.edu>

**Contact person:** DMD Conference

16th Annual Design of Medical Devices Conference, April 10-13, 2017. The world's largest medical device conference will be held at The Commons Hotel & McNamara Alumni Center, located on the University of Minnesota Twin Cities Campus.

**Organized by:** University of Minnesota  
**Deadline for abstracts/proposals:** 1st November 2016

## 12th Radiotechnology Congress and Training Seminars with International Participation

### Conference

27th to 30th April 2017  
Antalya, Turkey

**Website:** <http://2017.tmrtdr.org.tr/en/>

**Contact person:** Huseyin Ozan Tekin

12th Radiotechnology Congress aimed to gather technicians, scientists, researchers and academicians of Medical Radiation fields such as Radiology, Nuclear Medicine, Radiotherapy, Radiation Protection Nuclear Physics.

**Organized by:** Turkish Association of Medical Radiotechnology (TMRT-DER)

**Deadline for abstracts/proposals:** 5th March 2017

## NURSING AND HEALTH CARE '17 / International Conference on Nursing and Health Care

### Conference

24th to 25th March 2017  
Istanbul, Turkey

**Website:** <http://www.dakamconferences.org/nursingandhealthcare>

**Contact person:** Ozgur Ozturk

Papers will be published in DAKAM's online library and in the proceedings e-book (with an ISBN number), which will be given to you in a DVD box and will be sent to be reviewed in the "Thomson & Reuters WOS' Conference Proceedings Citation Index-CPCI"



## 2017 IEEE International Symposium on Biomedical Imaging (ISBI)

### Call for Abstracts and Non-Author Registration Now Open

## 1 Page Abstract Submission Now Open!!!

### Instructions for Authors

- Prepare a 1-page abstract of your work. Use the first page from these [templates](#).
- Abstracts are submitted [online](#). Follow the link, find ISBI2017 in the table. Select 'Submit a contribution to ISBI 2017', Submit a 1-page abstract.
- Abstracts will be reviewed for suitability by selected members of the Program Committee and will include a subset of the Scientific Review Committee to ensure that proper expertise is provided.

Upon acceptance of the abstract:

- Authors will prepare a poster presentation following the posted guidelines.

Submit a Paper via Papercept

---

## Attendee (non-authors) Registration Now Open

Non-Author Registration

---

Visit the ISBI 2017 Website

Connect with us

